INTERNATIONAL STUDIES IN THE FIELD OF

CHEMICAL ENGINEERING

MARCH 2026

EDITOR

Prof. Dr. Nil ACARALI

gece kitaplığı

İmtiyaz Sahibi / Yaşar Hız
Yayına Hazırlayan / Gece Kitaplığı

Birinci Basım / Mart 2026 - Ankara
ISBN / 978-625-321-013-7

Gece Kitaplığı
Kızılay Mah. Fevzi Çakmak 1. Sokak
Ümit Apt No: 22/A Çankaya/ANKARA
0312 384 80 40
www.gecekitapligi.com / gecekitapligi@gmail.com

Baskı & Cilt
Bizim Büro
Sertifika No: 42488

INTERNATIONAL STUDIES IN THE FIELD OF CHEMICAL ENGINEERING

MARCH 2026

EDITOR

Prof. Dr. Nil ACARALI

gece kitaplığı

CONTENTS

CHAPTER 1

ABSORBENT MATERIALS FROM CONVENTIONAL SYSTEMS TO NANOMATERIALS AND RADAR ABSORBING TECHNOLOGIES

Ayça Ceren ÇAM[1], Fatma İrem ŞAHİN[2], Nil ACARALI[3]

1 Chemical Engineer, Yildiz Technical University, Department of Chemical Engineering, 34220, Esenler-İstanbul, Türkiye. 0009-0001-0360-5676
2 Chemical Engineer, Yildiz Technical University, Department of Chemical Engineering, 34220, Esenler-İstanbul, Türkiye. 0000-0001-7670-8871
3 Prof.Dr. Yildiz Technical University, Department of Chemical Engineering, 34220, Esenler-İstanbul, Türkiye. 0000-0003-4618-1540 nilbaran@gmail.com

1. INTRODUCTION

Fluids are retained and absorbed by using absorbents [1]. Absorption is defined as penetration of water or other liquids into solid substances pores [2]. An ideal absorbent has a fast rate and good capacity of absorption, long-term holding capacity [3]. Absorbents are used in many different industries with variable objectives [4]. Depending on their structural form and chemical composition, absorbents could be classified into several material groups, among which foams represent one of the most widely used categories. Foam is used as an absorbent in different industries. There are many types of foams in the world like open and closed-cell foams, cross-linked polyethylene foams, PVC foams, polyurethane, polyether foam, polyester foam, ethafoam, rubber foams [5]. Open-celled hydrophilic polymeric foams offer capillary fluid absorption [6]. In addition to polymer-based absorbents, naturally occurring inorganic materials have also attracted significant attention due to their availability and surface characteristics. Clays and clay minerals play a significant role in geology, industry, agriculture, as well as the building of buildings, bridges, dams, and other constructions [7]. Smectites are known to be often very thin flakes with extremely small particle sizes, resulting in a material with a large surface area [8]. Diatomites are lightweight and highly porous materials primarily composed of siliceous skeletal remains of microscopic diatoms. Owing to their pronounced liquid absorption capability, diatomites are widely employed as effective for a variety of substances and formulations [9]. There are many different types of absorbents. These absorbents could be categorized based on the materials they absorbed. Oil, noise, and CO_2 could be given as materials possible to be absorbed [10]. Among these categories, oil absorbents have gained particular importance due to the scale and environmental impact of the petroleum industry. With the performance and volume of the oil industry, it is practically impossible to use oil without causing loss [11]. Previous oil tanker accidents have seriously contaminated the ocean [12]. Oil present in industrial wastewater is also a concern for the ecosystem [13]. Materials made of oil-absorbing polymers have high oil retention capability [14]. The term noise pollution describes the increase in ambient noise levels brought on by human activity [15]. Sound-absorbing asphalt could be used to solve the problem [16]. Similarly, gaseous pollutants have become a major focus of absorbent material research due to global environmental concerns. Several significant sectors produce substantial amounts of carbon dioxide [17]. Three different kinds of commercially accessible materials are mainly used, and some of them allow exhaled anesthetic chemicals to be rebreathed [18, 19]. A possible effective absorbent for removing CO_2 from post-combustion exhaust gases is 2-Aminoethylethanolamine [20]. In addition to environmental pollutants, absorbent materials are also developed to protect materials and

human health from radiation-related degradation. Sunlight's ultraviolet radiation causes rapid photodegradation of organic polymers is harmful to human health [21]. The development of biodegradable biological materials with UV absorption properties has generated significant interest [22]. It was reported that particles with a high specific surface area could dramatically increase the degree of otherwise unfavourable kinetic or thermodynamic processes [23]. As a result of the spilling in oil and chemical compound leaks and countless animals [24]. These criteria motivated the quest for novel absorber materials [25]. Recent research efforts have therefore focused on engineered and bio-based absorbents with enhanced performance. Cellulose-based superabsorbent is formed by bacterial cellulose on grafting acrylic acid with a crosslinker and ammonium persulfate as an initiator [26]. Polymer solid foams are crucial materials that were frequently employed in current technologies as extremely efficient absorbents [27]. Overview of absorbent materials and nano-absorbent technologies were shown in Figure 1.

Figure 1. Overview of Absorbent Materials and Nano-Absorbent Technologies

To provide a structured overview of the wide range of absorbent materials discussed in this chapter, their industrial usage, application areas, and key performance characteristics were systematically summarized in Table 1.

Table 1. Summary of Absorbent Materials: Usage, Applications, and Key Characteristics

Category	Material Usage	Applications	Key Characteristics	Reference
Absorbents	Various	Retaining fluids in various sectors	Absorbents must have high absorption rate, capacity, and retention time.	[1-3]
Chemical Absorbents	Natural minerals, polymers,	Cleanup of chemical spills	Quick and effective absorption, reusable, and specific to chemical properties	[4]
Foam Absorbents	Polyurethane	Construction, insulation, absorbent products	Must resist aggressive materials; open-celled hydrophilic foams in high-performance absorbent cores	[5, 6]
Clay Absorbents	Smectite	Pet litter, herbicides, petroleum, water absorption	Known as "swelling clay"; high absorption capacity due to large surface area	[8]
	Sepiolite	Various industrial applications	Effective due to charge on pores and large surface area	[7]
	Diatomite	Filtration, sorbents, fillers, nanocomposites	Excellent retaining medium; wide range of applications	[9]
Oil Absorbents	Biomass-derived materials	Oil spill cleanup, industrial wastewater treatment	High oil retention capability but limited by surface alteration and high-temperature carbonization.	[14]
Noise Absorbents	Bituminous conglomerate	Reduces noise and aids rainwater drainage	Draining layer acts as a sound-absorbing septum	[16]
CO_2 Absorbents	Lithium hydroxide, Sodasorb, Baralyme	CO_2 capture in various applications	High efficiency in CO_2 absorption; in anaesthesia and flue gas treatment	[17-20]
UV Absorbents	Triazine, zinc oxide, titanium dioxide	UV protection for materials and health	Protects against UV radiation; organic and inorganic options available with varying effectiveness	[21, 22]

2. NANOMATERIALS IN INDUSTRIES AND NANOMATERIAL BASED ABSORBENTS

In response to the limitations of conventional absorbent materials, recent research has increasingly focused on materials engineered at the nanoscale [28]. Nanomaterials had special and specific characteristics because of their small dimensions and large surface area [29]. Nanomaterials could enter the body via the skin, even if it was unbroken, as well as by inhalation or ingestion [30]. Nanoparticles manufactured in a variety of ways with physical approaches and chemical processes being the most common [31]. Nanomaterials were increasingly pervasive in daily life and were slowly being sold as commodities [32]. Parallel to their growing commercial availability, nanomaterials have become essential components in addressing large-scale industrial and energy related challenges. The rise in global energy consumption was accelerated the development of innovative technology in hydrocarbon recovery techniques [33]. Obtaining materials with the needed qualities was one of the most difficulties in contemporary processes [34]. Metal nanoparticles were remarkable due to extraordinary optical, catalytic, and electrical properties [31, 35]. These advantageous properties enabled the widespread integration of nanotechnology into advanced industrial systems. Nanotechnology was used in a wide range of communications and electronic industrial products [36]. Beyond electronics, nanomaterials have become integral to modern transportation and manufacturing technologies. Due to a wide variety of these gadgets formed on flexible supports on a large scale, printed electronics also known as PE were employed in the fabrication of electronic devices [37, 38]. Automobile production contained several components made of nanomaterials that were integrated to make the cars [39]. Overall, nanotechnology represented a transformative scientific and technological paradigm on industrial development and material design. Nanotechnology was a pioneering scientific and technical idea that had a significant influence on people life [23].

3. RADAR

As an extension of nanomaterial-based absorbent technologies, radar absorbing materials represented a specialized class of absorbents designed for electromagnetic energy attenuation rather than fluid or gas retention. Since radar's creation, techniques for lowering microwave reflections investigated since it was a sensitive detecting instrument [40]. The electromagnetic waves were important in daily lives which reflected energy acting on the matter in the form of electromagnetic fields [41]. In this context, absorption referred to the dissipation of electromagnetic energy within a material rather than its reflection back to the source. As illustrated in Figure 2, incoming radar waves interacted with radar absorbing materials (RAMs),

where electromagnetic energy was attenuated through absorption mechanisms and converted into thermal energy, resulting in minimal reflection.

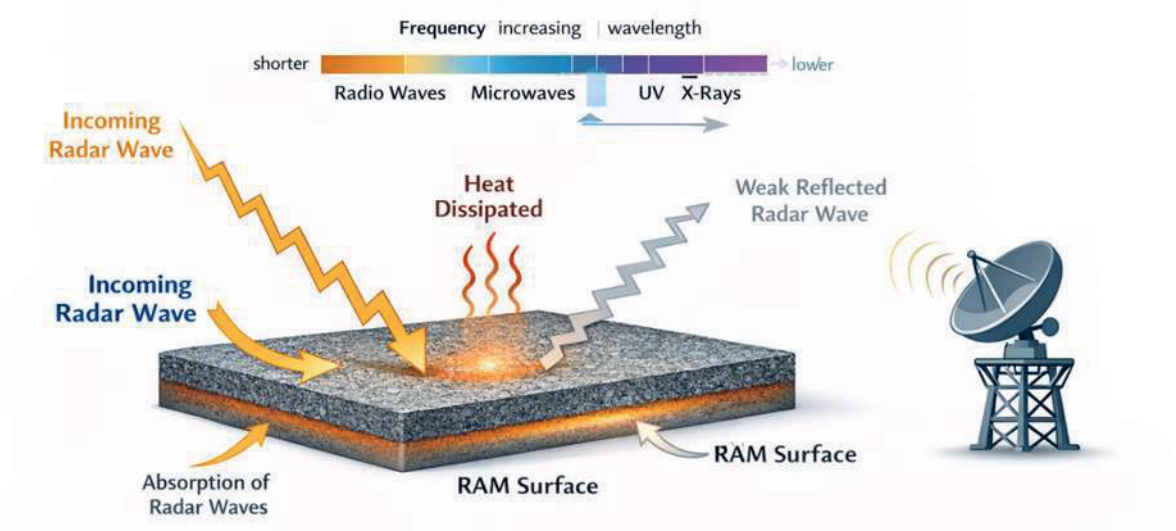

Figure 2. Principle of Radar Wave Absorption Using Radar Absorbing Materials (RAMs)

Radar absorbing materials (RAMs) research was established by the 1930s, driven primarily by military and strategic needs to reduce electromagnetic wave reflection and radar detectability [42]. Understanding the fundamental interaction between electromagnetic waves and material properties formed the basis of early RAM research. Early studies focused on understanding the interaction between incident microwave radiation and material properties such as electrical conductivity, magnetic permeability, and dielectric permittivity. Over time, this research evolved into a multidisciplinary field combining materials science, electromagnetics, and applied physics. An ideal RAM was expected to possess several critical characteristics, including high electromagnetic wave attenuation efficiency over a broad frequency range, low density, minimal thickness, mechanical durability, thermal stability, and environmental resistance [43]. Radar absorption could be achieved using a wide variety of materials, including metals and metal particles, ferrites, conductive polymers, carbon-based materials, and dielectric composites [44]. Carbon-based absorbent systems attracted considerable interest because of their low density, adjustable electrical characteristics, and economic viability. Structural design strategies introduced to further improve absorption efficiency. Multilayer absorber designs developed to enhance absorption performance, where double-layer structures incorporating carbon black and fibrous carbon provide synergistic effects by combining dielectric and conductive loss mechanisms [45]. Furthermore, radar-absorbing materials were not limited to

stealth or military platforms, it was integrated as complementary solutions alongside conventional electromagnetic shielding techniques in electronic equipment [46] (Table 2).

Table 2. Radar Absorbing Materials (RAMs): Summary of Techniques and Applications

Study	Materials	Applications	Findings	Reference
Conducting Polymers	Polyaniline	Cost-effective, modifiable absorbers	Polyaniline's derivatives offer opportunities to adjust absorber characteristics	[39]
Radar Absorbing Materials	Metals, metal particles, ferrites, conductive polymers, dielectric materials	Anechoic chambers, radar reflection reduction	Absorb electromagnetic waves and convert them to thermal energy; ideal RAMs are thin, light	[40, 41]
Military Applications	Various RAMs	Radar invisibility for military platforms	RAM reduces radar visibility and detection range	[44]
Double Layers	Carbon black, fibrous carbon	Enhanced absorption properties	Improved absorption through layered structures	[45]
Dual-Use Technology	Various RAMs	Defence applications	RAMs have potential for industrial and residential use, reducing resonance phenomena	[42, 46]

4. ANALYSIS AND EVALUATION

Following the discussion of absorbent materials, nanotechnology-based systems, and radar absorbing applications, this section focused on selected experimental studies that demonstrate practical implementations of absorbent technologies. By research and chromatographic condition optimization, an HPLC technique for the detection of 11 different UV absorbents in plastic food contact materials developed by researchers [47]. In addition to analytical detection techniques, absorbent materials are investigated in consumer-oriented applications. Another research [48] examined the many ingredients found in commercial shoes, contribution to improving and strengthening their operations, and the desirable qualities for best performance. In a study [49], it had been mentioned that heavy metal ions in industrial effluent were effectively absorbed by cement-based products. According to the findings, the compressive strength of absorbent particle was strongly connected with cement concentration and curing age. An antibacterial smart absorbent pad [50] with a Janus structure was formed to maintain and reflect the meat's quality. To provide a comparative perspective on these diverse research

efforts, a concise overview of recent literature on absorbent materials and techniques is presented in Table 3.

Table 3. Overview of Recent Research on Absorbent Materials and Techniques

Study	**Reference**	**Materials & Techniques**	**Findings**	**Applications**
Clay Bed Usability	[2]	Absorbent clay beds, Ca-Na bentonite	Investigated absorption and mechanical property changes due to heat treatment	Cat litter production, clay treatment
CO_2 Adsorption	[17]	Magnetic mesoporous silica-based nano-absorbent	High stability, reusability, and selectivity for CO_2 capture	Large-scale CO_2 capture in energy and industrial sectors
UV Absorbent Film	[22]	UV absorbent film, grape syrup, PLA matrix	UV-Vis studies showed absorption of UV radiation	UV protection in films, potentially for packaging.
Nanostructured RAMs	[43]	Nanostructured RAMs, magnetic-dielectric absorbers	Improved absorption properties due to nanoscale size	Microwave absorption in RAMs
UV Absorbent Detection	[47]	HPLC technique, UV absorbents	Successfully separated 11 UV absorbents in less than 30 minutes	Detection of UV absorbents in plastic food contact materials
Shoe Material Analysis	[48]	Commercial shoe ingredients, organic and carbon nanomaterials	Evaluated materials for performance improvements	Shoe manufacturing
Heavy Metal Absorption	[49]	Cement-based products, coke, porous absorbent	Effective absorption of heavy metal ions	Industrial effluent treatment, heavy metal removal
Antibacterial Smart Pad	[50]	Janus structure pad, PU nanofibers, PVA nanofibers	Absorbs fluids, maintains dryness, inhibits bacterial growth	Meat preservation, freshness monitoring

5. CONCLUSIONS AND FUTURE PERSPECTIVES

The chapter provided an overview of absorbent materials employed across various industrial sectors, with particular emphasis on the importance of application specific material selection. The chapter also reviewed the growing importance of nanomaterials in absorbent technologies. Nanomaterials were shown to enhance absorption efficiency and functionality in many industrial sectors, offering new possibilities for performance improvement and material design. In parallel, radar absorbing materials were discussed as a specialized class of absorbents that operate on electromagnetic waves rather than fluids or gases. Their role in radar systems used for detection, monitoring, tracking, and targeting, particularly in military applications, was emphasized, demonstrating how absorption principles extend beyond conventional industrial contexts. Chemical applications represented one of the most critical areas for absorbent use, where rapid and effective absorption is essential for safety and environmental protection. Advances in nanotechnology continue to form new industrial opportunities suggesting that sustained investment in nano absorbent research will be important for future technological progress. Overall, the findings indicated that correct selection and application of absorbent materials could play a key role in mitigating the impacts of chemical spills and industrial waste. Continued research, combined with increased awareness and proper training for individuals working with hazardous substances, would contribute significantly to the responsible application of absorbents and the reduction of environmental and human health risks.

REFERENCES

Dawn, F. S.; Correale, J. V. Absorbent Product and Articles Made Therefrom. (1982) Document ID 19840003690.

Demirel, H.; Karapinaran, A. K. Use of Bentonite and Other Clays as Absorbents, Industrial Raw Materials Symposium. (1995) pp. 21-22.

Nguyen, D. C.; Bui, T. T.; Cho, Y. B.; Kim, Y. S. Preparation of a Highly Porous Clay-Based Absorbent for Hazard Spillage Mitigation via Two-Step Expansion of Vermiculite, *Minerals*. 2021, 11. https://doi.org/10.3390/min11121371

Jang, J.; Kim, B. S. Studies of Crosslinked Styrene-Alkyl Acrylate Copolymers for Oil Absorbency Application. II. Effects of Polymerization Conditions on Oil Absorbency, *J. Appl. Polym. Sci*. 2000, 77(4), 914–920.

Sabbahi, A.; Vergnaud, J. M. Absorption of Water by Polyurethane Foam. Modelling and Experiments, *Eur. Polym. J*. 1993, 29, 1243–1246.

Steckle, W. P.; Smith, M. E.; Sebring, R. J.; Nobile, A. Optimization of HIPE Foams, *Fusion Sci. Technol*. 2004, 45, 74–78. https://doi.org/10.13182/FST04-A430

Murray, H. H. Overview—Clay Mineral Applications, *Appl. Clay Sci*. 1991, 5(6), 379–395. https://doi.org/10.1016/0169-1317(91)90014-Z

Altaner, S. P. Smectite Group, Encyclopedia of Sediments and Sedimentary Rocks, Encyclopedia of Earth Sciences Series, Springer, Dordrecht. (1978) pp. 1120–1124. https://doi.org/10.1007/978-1-4020-3609-5_216

Ivanov, S. É.; Belyakov, A. V. Diatomite and its Applications, *Glass Ceram*. 2008, 65(1), 48–51. https://doi.org/10.1007/s10717-008-9005-6

Phạm, V. H.; Dickerson, J. H. Superhydrophobic Silanized Melamine Sponges as High Efficiency Oil Absorbent Materials, *ACS Appl. Mater. Interfaces*. 2014, 6(16), 14181–14188. https://doi.org/10.1021/am503503m

Zhao, J.; Xiao, C.; Yan, F.; Xu, N. A Review: Polymethacrylate Fibers as Oil Absorbents, *Polym. Rev*. 2013, 53(4), 527–545. https://doi.org/10.1080/15583724.2013.828749

Teas, C.; Kalligeros, S.; Zanikos, F.; Stournas, S.; Lois, E.; Anastopoulos, G. Investigation of the Effectiveness of Absorbent Materials in Oil Spills Clean Up, *Desalination*. 2001, 140(3), 259–264. https://doi.org/10.1016/S0011-9164(01)00375-7

Gupta, S.; Tai, N. Carbon Materials as Oil Sorbents: A Review on the Synthesis and Performance, *J. Mater. Chem*. A Mater. Energy Sustain. 2016, 4(5), 1550–1565. https://doi.org/10.1039/c5ta08321d

Zhang, T.; Li, Z.; Lu, Y.; Liu, Y.; Yang, D.; Li, Q.; Qiu, F. Recent Progress and Future Prospects of Oil-Absorbing Materials, *Chin. J. Chem. Eng*. 2019, 27(6), 1282–1295. https://doi.org/10.1016/j.cjche.2018.09.001

Slabbekoorn, H. Noise Pollution, *Curr. Biol*. 2019, 29(19), 1-4. https://doi.org/10.1016/j.cub.2019.07.018

Ciaburro, G.; Iannace, G.; Ali, M. E. A.; Alabdulkarem, A.; Nuhait, A. An Artificial Neural Network Approach to Modelling Absorbent Asphalts Acoustic Properties, *J. King Saud Univ. Eng. Sci*. 2021, 33(4), 213–220. https://doi.org/10.1016/j.jksues.2020.07.002

Liu, Z.; Du, Z.; Zou, W.; Li, H.; Mi, J.; Zhang, C. Easily Collected Nano-Absorbents for Carbon Dioxide Capture, *Chem. Eng. J*. 2013, 223, 915–920. https://doi.org/10.1016/j.cej.2012.12.017

Wang, T. C. Temperature Effects on Baralyme, Sodasorb, and Lithium Hydroxide, *Ind. Eng. Chem. Process Des. Dev*. 1975, 14(2), 191–193.

Feldman, J. M.; Hendrickx, J. F. A.; Kennedy, R. C. Carbon Dioxide Absorption during Inhalation Anesthesia: A Modern Practice, *Anesth. Analg*. 2021, 132(4), 993–1002. https://doi.org/10.1213/ane.0000000000005137

Kim, I.; Svendsen, H. F. Heat of Absorption of Carbon Dioxide (CO_2) in Monoethanolamine (MEA) and 2-(Aminoethyl)ethanolamine (AEEA) Solutions, *Ind. Eng. Chem. Res*. 2007, 46(17), 5803–5809. https://doi.org/10.1021/ie0616489

Feng, Y.; Li, D.; Yuan, W.; Evans, D.G.; Duan, X. Synthesis and characterization of a UV absorbent-intercalated Zn–Al layered double hydroxide. *Polym. Degrad. Stab.* 2006, 91, 789–794. https://doi.org/10.1016/j.polymdegradstab.2005.06.006

Nikvarz, N.; Khayati, G.R.; Sharafi, S. Preparation of UV absorbent films using polylactic acid and grape syrup for food packaging application. *Mater. Lett.* 2020, 276, 128187. https://doi.org/10.1016/j.matlet.2020.128187

Luther, W. Technological Analysis, Industrial Application of Nanomaterials – Chances and Risks. Future Technologies Division of VDI Technologiezentrum GmbH, Germany. *Tech. Rep.* 2004, 54, 1–112.

Zhang, T.; Yu, M.; Huang, Y.; Tan, J.; Zhang, M.; Zhu, X. Design and manufacturing of cost-effective tannin-based polyurethane foam as an efficient and reusable absorbent for oil and solvents. *Ind. Crops Prod.* 2022, 189, 115815. https://doi.org/10.1016/j.indcrop.2022.115815

Anoshkin, I.V.; Campion, J.; Lioubtchenko, D.; Oberhammer, J. Freeze-Dried Carbon Nanotube Aerogels for High-Frequency Absorber applications. *ACS Appl. Mater. Interfaces* 2018, 10, 19806–19811. https://doi.org/10.1021/acsami.8b03983

Luo, M.; Li, H.; Huang, C.; Zhang, H.; Xiong, L.; Chen, X.; Chen, X. Cellulose-Based Absorbent Production from Bacterial Cellulose and Acrylic Acid: Synthesis and Performance. *Polymers* 2018, 10, 702. https://doi.org/10.3390/polym10070702

Löffler, R.J.G.; Hanczyc, M.M.; Górecki, J. A camphene-camphor-polymer composite material for the production of superhydrophobic absorbent microporous foams. *Sci. Rep.* 2022, 12, 12243.

Datta, D.; Das, K.P.; Deepak, K.S.; Das, B. Candidates of functionalized nanomaterial-based membranes. *Elsevier EBooks* 2022, 81–127. https://doi.org/10.1016/b978-0-323-85946-2.00004-7

Kangas, H.; Pitkänen, M. Nanomaterials in Industry—How to Assess the Safety? *Ind. Appl. Nanomater.* 2019, 1–27. https://doi.org/10.1016/b978-0-12-815749-7.00001-3

Haynes, H.; Asmatulu, R. Nanotechnology safety in the aerospace industry. *Elsevier EBooks* 2013, 85–97. https://doi.org/10.1016/b978-0-444-59438-9.00007-2

Kaviarasu, C.; Ravichandran, M. Nanomaterials through Powder Metallurgy: Production, Processing, and Potential Applications toward Energy and Environment. *Springer EBooks* 2020, 1–40. https://doi.org/10.1007/978-3-030-11155-7_127-1

Talebian, S.; Rodrigues, T.; Neves, J.D.; Langer, R.; Conde, J. Facts and figures on materials science and nanotechnology progress and investment. *ACS Nano* 2021, 15, 15940–15952.

Bou-Hamdan, K.F. Applications of nanomaterials in the oil and gas industry. *Adv. Chem. Mater. Eng. Ser.* 2022, 173–198. https://doi.org/10.4018/978-1-7998-8936-6.ch008

Borodianskiy, K.; Zinigrad, M. Nanomaterials Applications in modern metallurgical processes. *Diffus. Found.* 2016, 9, 30–41. https://doi.org/10.4028/www.scientific.net/df.9.30

Tsutsui, T. Recent Technology of Powder Metallurgy and Applications. *Hitachi Powdered Metals Tech. Rep.* 2012, 54, 12–20.

Akujuobi, C.M. Nanotechnology safety in the electronics and telecommunications industries. *Elsevier EBooks* 2013, 141–159. https://doi.org/10.1016/b978-0-444-59438-9.00011-4

Bissessur, R. Nanomaterials applications. *Elsevier EBooks* 2020, 435–453. https://doi.org/10.1016/b978-0-12-816806-6.00018-2

Yang, Y.; Yang, X.; Tan, Y.; Yuan, Q. Recent progress in flexible and wearable bio-electronics based on nanomaterials. *Nano Res.* 2017, 10, 1560–1583. https://doi.org/10.1007/s12274-017-1476-8

Asmatulu, R.; Nguyễn, P.A.T.; Asmatulu, E. Nanotechnology safety in the automotive industry. *Elsevier EBooks* 2013, 57–72. https://doi.org/10.1016/B978-0-444-59438-9.00005-9

Saville, P. Review of Radar Absorbing Materials. *Def. R&D Can.-Atlantic* 2005, 5–15.

Ruiz-Perez, F.; López-Estrada, S.M.; Tolentino-Hernandez, R.V.; Caballero-Briones, F. Carbon-based radar absorbing materials: A critical review. *J. Sci. Adv. Mater. Devices* 2022, 7, 100454. https://doi.org/10.1016/j.jsamd.2022.100454

Vinoy, K.J.; Jha, R.M. Trends in radar absorbing materials technology. *Sadhana Acad. Proc. Eng. Sci.* 1995, 20, 815–850. https://doi.org/10.1007/BF02744411

Wang, Y.; Li, T.; Zhao, L.; Hu, Z.; Gu, Y. Research progress on nanostructured radar absorbing materials. *Energy Power Eng.* 2011, 3, 580–584. https://doi.org/10.4236/epe.2011.34072

Aktaş, G.; Aktaş, A.; Gürü, M. Effect of Paint Properties on Radar Absorption Capacity. *J. Fac. Eng. Archit. Gazi Univ.* 2016, 31, Article ID 59681. https://doi.org/10.17341/gummfd.59681

Zhukov, P.A.; Kirillov, V.Yu. The use of radar absorbing materials for electronic devices. *Proc. Int. Youth Conf. Radio Electron. Electr. Power Eng. (REEPE)* 2020, 1–5. https://doi.org/10.1109/reepe49198.2020.9059210

Kurniawan, A.F.; Anwar, M.S.; Nadiyyah, K.; Mashuri, M.; Triwikantoro, T.; Darminto, D. Thickness optimization of a double-layered microwave absorber combining magnetic and dielectric particles. *Mater. Res. Express* 2021, 8, 065001. https://doi.org/10.1088/2053-1591/ac04ea

Qiu, Y.; Zhang, Q.; Yang, Q.; Tan, C.; Zhang, L. Determination of 11 kinds of ultraviolet absorbents in plastic food contact materials by high performance liquid chromatography. *J. Phys.* 2022, 2194, 012004. https://doi.org/10.1088/1742-6596/2194/1/012004

Selvaraj, S.K.; Ramesh, R.; Narendhra, T.M.V.; Agarwal, I.N.; Chadha, U.; Paramasivam, V.; Palanisamy, P. New developments in Carbon-Based nanomaterials for automotive brake pad applications and future challenges. *J. Nanomater.* 2021, Article ID 6787435. https://doi.org/10.1155/2021/6787435

Cai, J.; Du, Y.; Zhang, R.; Tian, Q.; Xu, G.; Zhang, M. Preparation of cement-based absorbent with coke for Cr^{3+} removal. *Mater. Today Commun.* 2023, 35, 105749. https://doi.org/10.1016/j.mtcomm.2023.105749

Jiao, X.; Xie, J.; Du, H.; Bian, X.; Wang, C.; Zhou, L.; Wen, Y. Antibacterial smart absorbent pad with Janus structure for meat preservation. *Food Packag. Shelf Life* 2023, 37, Article ID 101066. https://doi.org/10.1016/j.fpsl.2023.101066

CHAPTER 2

SUSTAINABLE BIO-COMPOSITES FROM WASTE SUNFLOWER STALKS AND FOOD-BASED NATURAL BINDERS: A MECHANICAL AND PHYSICAL PROPERTIES ASSESSMENT

Duygu KURU[1], İrem BULGUR[2], Azra YUNUSOĞLU[3], Abdullah USLU[4], Sedef ÇELIK[5]

1 Associate Professor, Bilecik Seyh Edebali University, Faculty of Engineering, Department of Chemical Engineering, TR 11100 Bilecik, Türkiye, duygu.gokdai@bilecik.edu.tr, ORCID: 0000-0002-9727-5785
2 Bilecik Borsa Istanbul Science and Art Center, Bilecik, Türkiye ORCID: 0000-0001-8412-9183
3 Bilecik Borsa Istanbul Science and Art Center, Bilecik, Türkiye ORCID: 0009-0001-2201-5508
4 Bilecik Borsa Istanbul Science and Art Center, Bilecik, Türkiye ORCID: 0009-0003-7979-958X
5 Bilecik Borsa Istanbul Science and Art Center, Bilecik, Türkiye ORCID: 0000-0003-4793-3070

1. Introduction

Sunflower (*Helianthus annuus* L.), a member of the Compositae (Asteraceae) family, was first cultivated approximately 3,000 years ago in the regions of Arizona and New Mexico, North America. Recognized globally as a major agricultural crop, sunflower is primarily grown for their seeds and vegetable oil production. In addition to being the fourth-largest source of vegetable oil, sunflowers have historically served multiple purposes [1]. Early applications included the use of sunflower stalks and seeds in basketry, dye production, and medicinal practices [2]. From the 19th century onwards, the industrial production of sunflower oil and the commercial utilization of its by-products have increased substantially [3].

Sunflower stalks, owing to their favorable physical and chemical properties, represent a promising agricultural by-product for sustainable material production. Their low density (0.028 g/cm³) combined with high mechanical strength renders them attractive for construction material applications [4]. The outer region of the stem exhibits a higher Young's modulus, which enhances mechanical resistance and enables effective incorporation into composite materials [5]. Additionally, the high cellulose, hemicellulose, and lignin content of sunflower stalks facilitates their use as reinforcement agents in polymer composites [6]. These properties enhance their potential applications in areas such as bioremediation, particleboard production, and natural polymer composites.

According to 2024 data from the Turkish Statistical Institute (TÜİK), sunflower production in Turkey increased by 8.7% relative to the previous year, reaching approximately 2.4 million tons annually [7]. In Bilecik province specifically, sunflowers are cultivated both for oil and as a snack product, ranking as the third most widely grown crop after wheat and barley. Total production in Bilecik rose from 13,633 tons in 2022 to 18,398 tons in 2023 [8]. Currently, the seeds hold economic value and are commercialized, while the stems largely remain as waste. Historically, sunflower stalks in this region were employed for insulation, construction of hard surfaces, and mixed-soil ceilings; however, these traditional uses have largely disappeared. The potential for reusing sunflower stalks, combined with this historical knowledge, provides an inspiring foundation for exploring modern applications in the construction and building materials sector.

The development of composites derived from sunflower stalks is critical from both environmental and economic perspectives. Literature reports indicate that composites based on sunflower stalks can exhibit enhanced mechanical strength, impact resistance, and thermal stability [9]. For instance, Uğur et al. demonstrated a significant correlation between increased stalk content and water absorption and thickness swelling in particleboards fabricated from

sunflower stalks and wood particles [10]. Similarly, Sunmaz et al. reported that NaOH treatment improved the mechanical properties of bio-epoxy composites reinforced with sunflower shells [11]. Another study by Temiz et al. highlighted the promising performance of composites made from wood chips and other waste materials in sound and thermal insulation applications [12]. Moreover, ash derived from sunflower stalks has been suggested to enhance concrete resistance against freeze-thaw cycles and chemical attack, providing innovative solutions for the construction sector [9]. In a study conducted by Nimcharoen and colleagues, they obtained a biocomposite material from sunflower stems for use in wall panels. Natural latex was used as the binder in the study. They compared the outcomes of hot oven and hot compression treatments. Moisture content ranged from 6.01% to 14.20%, with only the 1:5 and 1:6 hot-compressed sunflower stalk composites exceeding 13%. Thickness swelling varied between 5.63% and 12.03%. All specimens demonstrated fire resistance meeting the UL94HB standard, classifying them as at least flame-retardant [13]. In particular, the inner core of sunflower stems (sunflower pith) stands out as a potential insulation material due to its porous structure and low density. However, its small size, irregular shape, and anisotropic properties limit its practical applications. The "crushing-stacking-molding" (BSM) technique, introduced to address this issue, consists of reducing sunflower pulp into small particles, impregnating them with phenol–formaldehyde (PF) resin, and subsequently molding the mixture into panels of specified dimensions and shapes. The biocomposites produced using this method exhibit superior properties, including mechanical strength, thermal insulation, and sound absorption. These biocomposites possess a thermal conductivity coefficient between 0.038 and 0.048 W m^{-1} K^{-1}, which decreases to 0.023 W m^{-1} K^{-1} when transformed into vacuum insulation panels. Additionally, 10 mm-thick SPF panels show a sound insulation coefficient of 0.34 across the 250–3000 Hz frequency range, indicating excellent suitability for sound absorption applications [14]. The study by Bekhta et al. focused on assessing the physical and mechanical characteristics of lightweight particleboards incorporating sunflower stalk particles in their core section. The study determined the density, water absorption, swelling, and bending properties of boards with different densities and compositions. The results showed that boards containing sunflower stalks offer an environmentally sustainable alternative, providing adequate mechanical performance and dimensional stability despite their low density. These findings support the potential use of agricultural waste as a valuable building material source [15].

This study presents an original approach that utilizes locally available sunflower stalks, an agricultural waste product, combined with natural binders to develop sustainable

construction materials, thereby enhancing the economic value of agricultural by-products and promoting environmentally friendly solutions. Although numerous studies in the literature have focused on synthetic binders, a comparative study on composite materials using natural binders has not been documented. Integrating the physical and mechanical properties of sunflower stalks into building materials offers substantial advantages over conventional alternatives. This approach not only serves as a model for waste management and resource efficiency but also contributes functionally to literature by advancing the development of low-cost, durable, and eco-conscious construction materials.

2. Materials and Methods

2.1. Materials

Sunflower (*Helianthus annuus* L.) stalks (Figure 1) were used as the primary raw material for the production of composites intended for construction material applications. The sunflower stalks utilized in this study were harvested in September 2024 from the fields of Taşçılar Village, a region where sunflower cultivation is widespread. The pith, a spongy substance located within the stalks, was removed, and the stalks were processed into coarse and fine particles. Subsequently, the particles were sieved and categorized into different size fractions: $\theta > 0.850$ mm, $0.600 > \theta > 0.425$ mm, $0.425 > \theta > 0.250$ mm, $0.250 > \theta > 0.090$ mm, and $\theta < 0.090$ mm.

For comparative purposes regarding mechanical performance, coarse sunflower stalk particles ($\theta \geq 0.600$ mm) and fine stalk extracts ($0.250 > \theta > 0.090$ mm) were selected. In the experimental study, these two particle types were combined with various binders, namely egg white, wheat starch, and epoxy resin, to fabricate the composite materials.

Figure 1. Sunflower stalk.

Egg white contains more than half of the niacin and riboflavin present in the whole egg, and the majority of the egg's carbohydrates are also found in the egg white. Approximately 63% of egg white consists of proteins, primarily ovalbumin. Due to its gelling properties and biocompatibility, egg white serves as an effective binder in composite materials. Its applications span a wide range of sectors, including ceramics, nanocomposites, and biomedical scaffolds, demonstrating both its versatility and environmental benefits.

Starch granules are primarily composed of glucose polymers, namely amylose and amylopectin, while also containing small amounts of phosphate and lipids. Due to its biodegradability and ability to enhance mechanical properties, starch serves as an effective binder in composite materials. In this study, starch was gelatinized with water before use, as gelatinization is essential for its function as a binder in composites.

Epoxy is a resinous material with increased viscosity that hardens to a stone-like consistency due to the additives it contains. It is commonly used as a binder in paints and various other mixtures. Epoxies are two-component systems that require mixing before application. In composite materials, epoxy serves as a crucial binder due to its unique properties, including high strength, elasticity, and resistance to thermal and chemical degradation.

2.2. Method

The sunflower stalks collected from the fields were initially left to dry in the sun for 15 days. Once dried, the pith, a spongy material within the stalks, was removed manually with a knife and ground for 15 minutes using a household blender. The ground spongy material was then sieved and

separated into different particle sizes. Small and large particle fractions were placed in separate containers to be combined with different binders.

The fine particle fraction was mixed with whisked liquid egg white as the binder. Once a homogeneous and viscous consistency was achieved, the mixture was poured into silicone molds and cured in an oven at 50 °C for approximately 3 hours. After cooling and standing at room temperature for 2 days, the composites were demolded. The same procedure was repeated for the coarse particle fraction with egg white.

This process was subsequently applied to the fine particle fraction using starch and epoxy, as well as to the coarse particle fraction, to produce the composite materials. Photographs of the resulting composites are provided in Figure 2.

Figure 2. Images of composites produced using different binders.

The procedures for producing the composites using the pre-prepared egg white, starch, and epoxy for the different formulations intended for analysis are summarized in Figure 3.

For the production of composite materials containing sunflower stalk extract, different ratios of egg white, starch, and epoxy were tested as binders to determine the most suitable formulations for the study. The resulting mixtures were poured into 20 silicone molds, each measuring 100 mm × 200 mm × 15 mm.

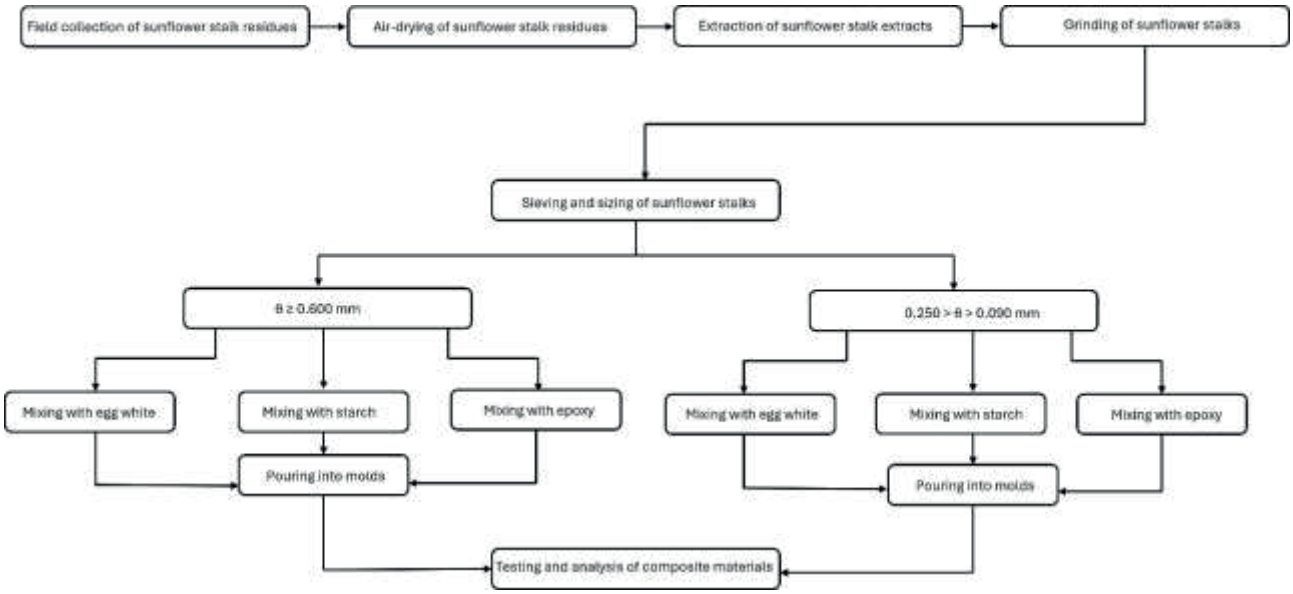

Figure 3. Composite production flow chart.

All mixtures were poured into molds of identical volume. Different ratios of the main material and binders were used in each composite preparation to achieve the desired density. The casting formulation used in the preparation of the composite material is given in Table 1.

Table 1. Casting formulation employed in the synthesis of composite materials

Sample Code	0.250>θ>0.090 (g)	θ≥0.0600 (g)	Egg white (g)	Starch (g)	Epoxy (g)	Water (g)
UY	75	-	55	-	-	-
UN	50	-	-	50	-	100
IY	-	70	65	-	-	-
IN	-	70	-	50	-	100
UE	100	-	-	-	75	-
IE	-	80	-	-	75	-

Codes were assigned to the composite samples for subsequent testing and analysis. The coding system is as follows: UY for samples prepared with egg white and fine sunflower stalk particles ($0.250 > \theta > 0.090$ mm), IY for samples with egg white and coarse sunflower stalk particles ($\theta \geq 0.0600$ mm), UN for samples with starch and fine particles ($0.250 > \theta > 0.090$ mm), IN for samples

with starch and coarse particles ($\theta \geq 0.0600$ mm), UE for samples with epoxy and fine particles ($0.250 > \theta > 0.090$ mm), and IE for samples with epoxy and coarse particles ($\theta \geq 0.0600$ mm).

2.3. Characterization

The morphological characteristics of the composite materials were examined using SEM (Zeiss Supra 40VP). The functional groups in the structure of composite materials were determined using FT-IR (Perkin Elmer / Spectrum 100) analysis. Flexural strength and modulus were evaluated through three-point bending tests conducted in accordance with EN ISO 178, using a Shimadzu AG-IC Test Machine at a crosshead speed of 2 mm·min^{-1}. Five specimens were tested in each group, and the corresponding mean values were recorded. All flexural tests were carried out at room conditions of 23 ± 2 °C. To determine the composites' mechanical behavior, rectangular samples measuring 100 mm in length, 10 mm in width, and 4 mm in thickness were used. The flexural strength (σ) and flexural strain (ε_f) of the composites were calculated using the following equations:

$$\sigma = ((3PL) / (2bd^2)) \quad (1)$$

$$\varepsilon_f = (6Dd) / (L^2) \quad (2)$$

where *L* is the support span (mm), *b* is the specimen width (mm), *d* is the specimen thickness (mm), *P* is the maximum applied load (N), and *D* represents the elongation at the midpoint of the sample.

According to ASTM D570, Archimedes' Principle was applied to determine the density of the composite specimens. Bulk density, thickness swelling, water absorption, and open porosity were among the physical properties investigated. Tests were conducted on 5 × 5 cm samples, and the corresponding properties were derived from the following formulas:

$$W_A \text{ (Water Absorption), \%} = ((W_3 - W_1) / W_1) * 100 \quad (3)$$

$$\text{bulk density} = (W_1 / (W_3 - W_2)) * 100 \quad (4)$$

$$\text{open porosity} = ((W_3 - W_1) / (W_3 - W_2)) * 100 \quad (5)$$

where W_1 is dry weight, W_2 is suspended weight, and W_3 is saturated weight.

Impact energy absorption of the composites was evaluated using an Izod impact testing device (DVT CD Devotrans Quality Control Test Instruments Ltd.) fitted with a 6 J hammer. The hammer descends at an angle of 150° with a speed of 3.8 m/s. The impact strength was obtained as follows:

$$\text{impact strength} = (\text{fracture energy, Joule}) / (\text{cross-sectional area, m}^2) \quad (6)$$

To measure the Shore D hardness (Hildebrand, Shore D, ASTM D 2240), a composite

specimen with an 8 cm diameter was positioned on a rigid, flat surface. The instrument's indentor was then pressed perpendicularly into the specimen's surface until it made firm contact. The hardness value was recorded within 1 second. For each composite formulation, three replicate tests were performed to obtain an average hardness value.

3. Results and Discussion

3.1. Structural Analysis of Composites

Figure 4 shows morphological images of composites obtained using different binders. When comparing fine and coarse particles, it is clearly observed that the composites obtained with coarse particles have more and larger pores.

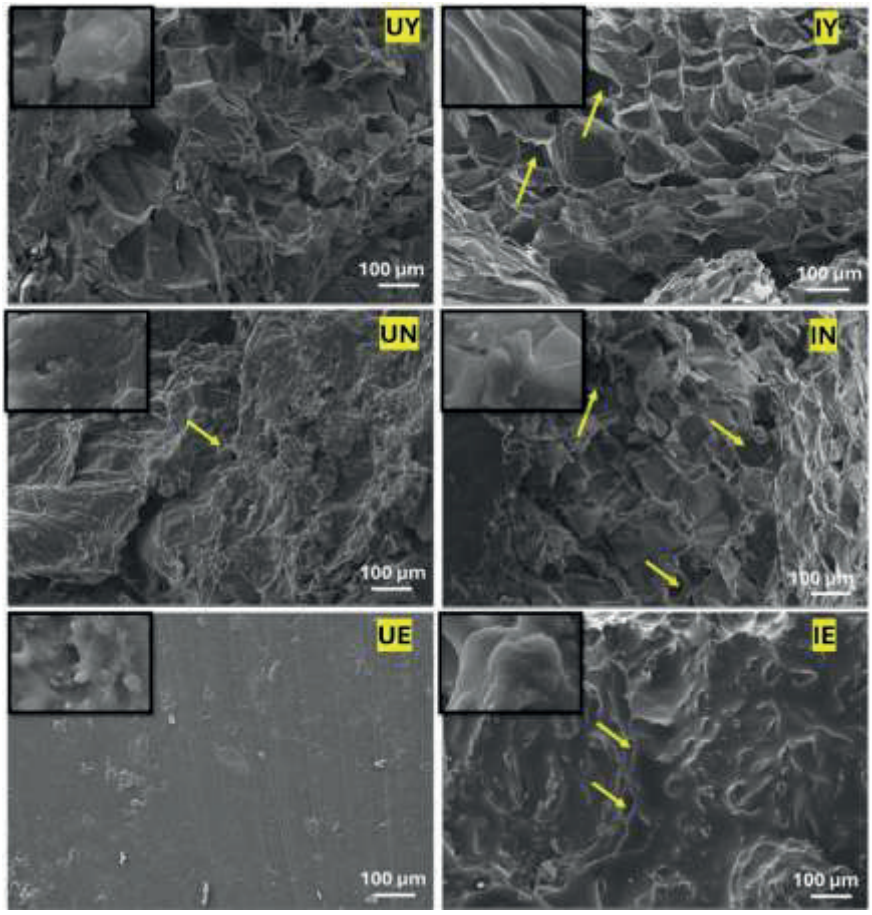

Figure 4. SEM images of composites synthesized under different conditions.

The most porous structure was observed in the composite using egg white binder and large sunflower stalk particles as filler. The presence of a loose, porous interface here indicates weak adhesion between the egg white and the sunflower, which also causes their mechanical properties to be weaker [16]. An examination of the composite structure formed from sunflower stalks and starch revealed a more homogeneous morphology compared to the egg-based counterpart. This is evidenced

by the strong interfacial contact between the matrix and filler phases, which consequently led to a reduction in porosity [17]. In the case where epoxy is used as a binder, the porosity is almost negligible, and the matrix and filler phases have achieved complete contact with each other; therefore, the structure is homogeneous. It confirms that the fibers are uniformly distributed within the composite and do not exhibit a tendency to agglomerate. Particle size also governs the efficiency of reinforcement: finer stalk particles provide a larger surface area for bonding and create a denser structure, while coarser particles tend to cluster and generate localized stress concentrations. Therefore, the morphology of sunflower stalks, particularly interfacial contact and porosity, directly determines the mechanical behavior of the composite material [18,19].

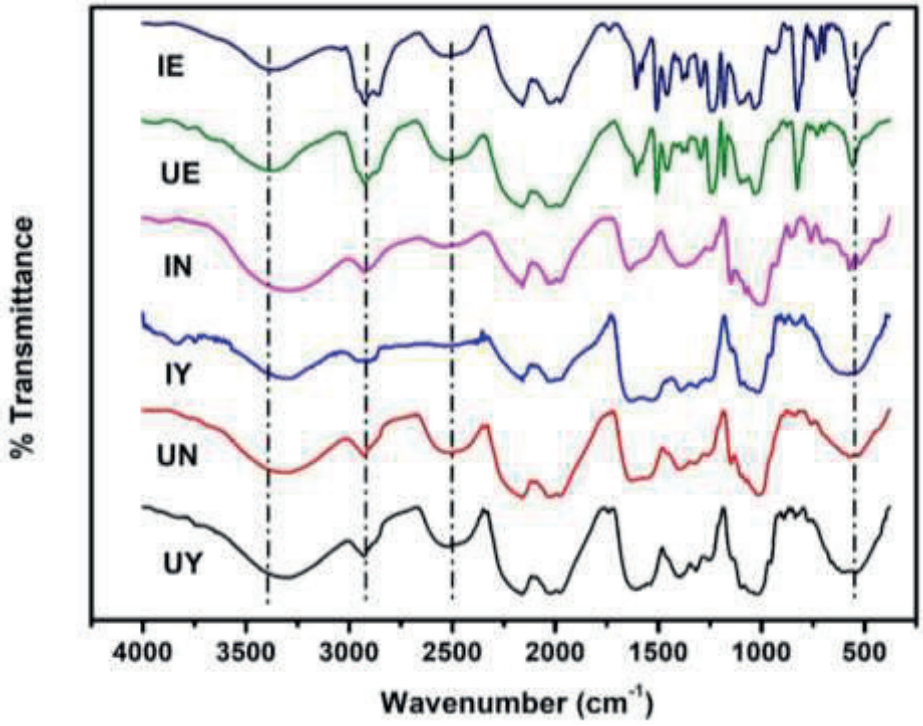

Figure 5. IR spectrum of composite materials.

Figure 5 presents the IR spectra of composites obtained under different conditions. In all composites, the stretching observed around 3380 cm^{-1} indicates the presence of water and hydrogen bonds, corresponding to the –OH stretching vibration. The characteristic band near 1020 cm^{-1} corresponds to the C–O–C stretching vibrations, representing the presence of cellulose and hemicellulose in the sunflower stalks. The stretching observed in the 1400–1500 cm^{-1} range is attributed to the C=C bonds in lignin. The band at 1611 cm^{-1} corresponds to the C=O group vibrations originating from lignin and pectin within the structure [20]. All composites exhibit characteristic functional groups of sunflower stalks. Notably, the composites prepared with epoxy show higher

stretching intensity compared to the others, primarily due to a more homogeneous distribution of the sunflower stalks within the epoxy matrix and reduced structural deformation [21].

3.2. Mechanical Properties of Composites

Based on the mechanical strength tests, it was observed that the specimens containing sunflower stalk extract particles with sizes in the range of 0.250>θ>0.090, bonded with starch and epoxy, exhibited higher flexural strength compared to those produced with other binders (Figure 6). The highest flexural strength was recorded for the specimen prepared with sunflower stalk extract particles of 0.250>θ>0.090 in size using epoxy as the binder.

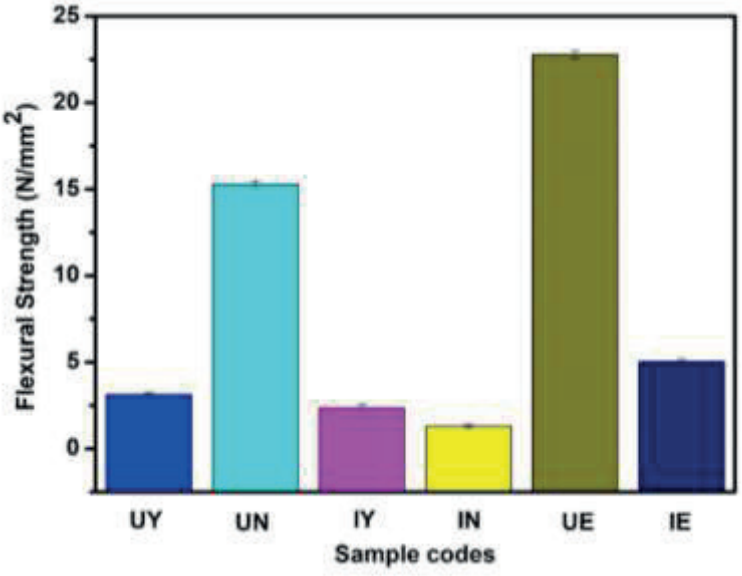

Figure 6. Flexural strength of composites.

The obtained results demonstrated that the use of sunflower stalk extract particles with sizes in the range of 0.250>θ>0.090 led to an improvement in flexural strength. This finding suggests that particle size has a direct influence on the mechanical properties of the material. The specified size range may have enabled more effective interaction between the particles and the binder, resulting in a more homogeneous structure and stronger interfacial bonding within the material [22]. This situation can also be clearly observed in the SEM analyses. Sanya et al. also demonstrated in their study on epoxy composites reinforced with silicon carbide that composites containing smaller silicon carbide particles exhibited superior flexural strength, compressive strength, and hardness values [23]. In another study, silicon carbide particles of varying sizes were embedded in an aluminum matrix, and their mechanical properties were compared. As particle size increased, compressive strength and impact resistance decreased [24]. In the study conducted by Efe and Hakkı, sunflower stalks were utilized to produce composite structures, and the flexural strength of these composites was found to range between 9 and 13 N/mm². Notably, the composites prepared using a starch-based binder in our

study approached this range, indicating that a natural material can serve as a viable alternative to conventional binders [25].

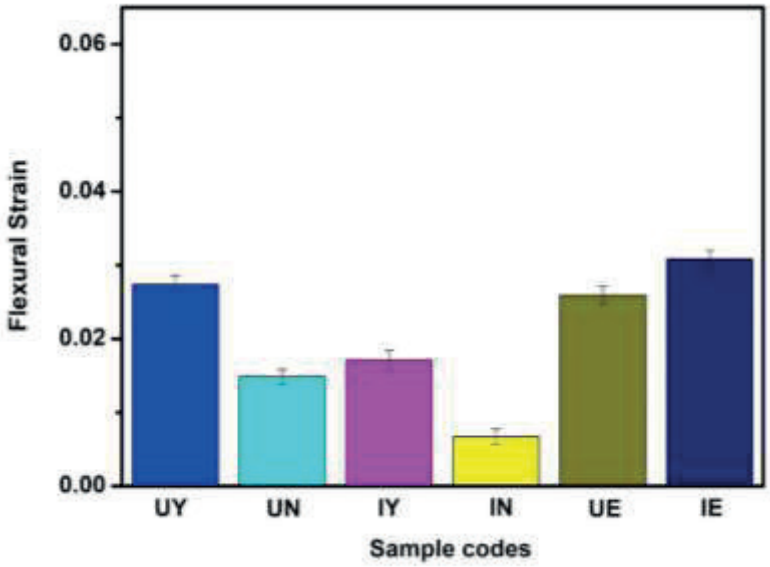

Figure 7. Flexural strain of composites.

In Figure 7, analysis of the flexural strain results of the composite materials revealed that an increase in flexural strain was observed in the specimens containing sunflower stalk extract particles larger than $\theta \geq 0.600$ bonded with epoxy, as well as those containing particles in the range of $0.250>\theta>0.090$ bonded with egg white. The highest flexural strain was recorded for the specimen prepared with $\theta \geq 0.600$ particles using epoxy as the binder.

These findings indicate that larger particles can enhance mechanical strength under certain conditions. When combined with a binder, larger particle sizes may provide greater load-bearing capacity within the internal structure of the material [26]. Large particles can reduce the formation of microcracks in the binder matrix and mitigate stress concentration during load transfer, thereby improving overall strength [27]. The observation that the highest flexural strain was achieved with the $\theta \geq 0.600$ + epoxy combination suggests that larger particles integrate more effectively with epoxy, forming a more robust structure in which the epoxy acts as a reinforcing matrix [28]. Conversely, the $0.250>\theta>0.090$ + egg white composite demonstrates that natural binders, such as egg white, can achieve high efficiency at the microstructural level with smaller particle sizes. However, this combination does not provide the same level of mechanical strength as the epoxy-based system. Izod impact strength and hardness values of the composites were given in Figure 8.

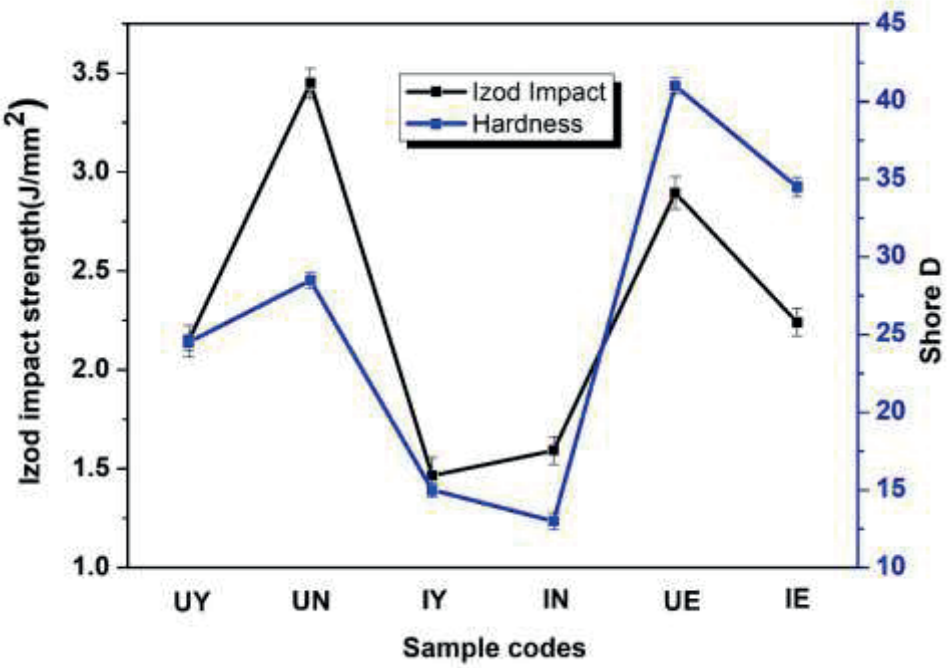

Figure 8. Izod impact strength and hardness values of composites.

Impact resistance tests performed on the composite materials revealed that specimens prepared with sunflower stalk extract particles in the size range of 0.250>θ>0.090, bonded with starch and epoxy, exhibited increased impact resistance. The highest impact resistance was observed in the specimen containing 0.250>θ>0.090 particles bonded with starch. These results suggest that the natural binder may contribute to enhancing the impact resistance of the composite material. Smaller particles can achieve stronger bonding with the binder due to their increased surface area. This enhanced interaction contributes to improved impact resistance, thereby enhancing the mechanical properties of the material [29]. The highest impact resistance was observed in the specimen prepared with starch as the binder, indicating that starch has a high capacity to reinforce the material matrix at this particle size. Ductile binders, such as starch, more effectively dissipate energy and slow crack propagation, thereby enabling higher impact strength. In contrast, brittle binders promote rapid crack initiation, resulting in reduced impact resistance [30].

Specimens prepared with epoxy also exhibited increased impact resistance, although their performance was not as high as that of the starch-bonded samples. In composites containing small sunflower stalk particles 0.250>θ>0.090, the type of binder played a critical role in determining impact resistance. The superior performance achieved with starch demonstrates that natural binders can be effective in enhancing mechanical performance. Moreover, the use of starch as a binder, which provides the highest impact resistance, presents a significant advantage for projects prioritizing

sustainability and environmental friendliness. Its natural and biodegradable nature further highlights the potential of this material for the development of green construction materials.

Hardness tests conducted on the composite materials revealed that specimens prepared with sunflower stalk extract particles of sizes $0.250>\theta>0.090$ and $\theta \geq 0.600$, bonded with epoxy, exhibited increased hardness. The highest hardness was observed in the specimen containing $0.250>\theta>0.090$ particles bonded with epoxy. This indicates that smaller particles interact more effectively with the epoxy binder, thereby reinforcing the binder matrix. Epoxy provided an increase in hardness for both particle sizes, demonstrating its capability to enhance the mechanical performance of composites across different particle size ranges.

3.3. Physical Properties of Composites

In the physical analyses of the composite materials, open porosity, water absorption, and thickness swelling were examined. The results obtained are presented in Table 2. The specimen bonded with epoxy and containing particles in the size range of $0.250>\theta>0.090$ exhibited the lowest porosity (3.86%), the lowest water absorption (10.50%), and the lowest thickness swelling (3.50%). This indicates that the epoxy binder provides excellent adhesion with the small particles ($0.250 < \theta < 0.090$), thereby minimizing void formation. It also demonstrates that the minimal presence of voids within the material structure, combined with the impermeable nature of the epoxy binder, contributes to its effectiveness. Moreover, the low porosity and water absorption properties suggest that the epoxy binder plays a crucial role in maintaining the material's stability [31]. The fibrous and porous structure of sunflower stalks allows them to easily absorb water.

Table 2. Physical properties of composite materials.

Sample code	Open porosity (%)	Water Absorption (%)	Thickness swelling (%)
UY	73.48	233.07	9.04
UN	62.23	159.66	5.79
İY	87.33	701.07	18.71
İN	86.34	644.79	6.01
UE	3.86	10.50	3.50
İE	39.90	33.06	13.33

SEM images indicate that the porous nature of the fibers and the presence of interfacial voids contribute to an increased water absorption capacity. However, a homogeneous distribution of fibers and well-bonded interfaces partially restricts water ingress, thereby reducing the overall water absorption rate as seen in epoxy-based composites [32]. The presence of interfacial voids and porosity allows water to accumulate between the fibers, leading to an increase in thickness swelling. Fiber size and distribution directly influence the swelling rate; small and homogeneously distributed fibers

result in less swelling, whereas large or clustered fibers can create localized swelling points. In the study by Migneault et al., composites reinforced with long fibers exhibited water absorption and swelling rates that were 51% and 46% higher, respectively, compared to composites containing shorter fibers. These results indicate that fiber length and distribution are critical factors influencing the swelling behavior of composites [33].

4. Conclusion and Suggestions

The mechanical and physical properties of sunflower stalk extract-based composites were strongly influenced by particle size and binder type. Flexural tests showed that particles in the $0.250>\theta>0.090$ range enhanced flexural strength due to improved interfacial bonding and more effective load transfer, while larger particles $\theta \geq 0.600$ bonded with epoxy exhibited the highest flexural stress, indicating strong mechanical interaction with the matrix.

Impact resistance was highest for composites containing $0.250>\theta>0.090$ particles with starch binder. The small particle size increased surface contact with the binder, promoting homogeneous stress distribution and efficient energy dissipation. Hardness tests revealed that the same particle range bonded with epoxy provided the highest hardness, highlighting the reinforcing effect of smaller particles within a rigid epoxy matrix. The morphology of sunflower stalks**,** particularly interfacial contact and porosity**,** directly determines the mechanical behavior of the composite material. In terms of physical performance, small particles with epoxy resulted in the lowest porosity, water absorption, and thickness swelling, demonstrating enhanced dimensional stability. Overall, the results suggest that optimizing particle size and binder type is crucial for strengthening mechanical performance and durability, with natural binders, such as starch, offering a sustainable option for impact-resistant composites. In particular, the use of starch-based composites as a sustainable alternative to synthetic binders underscores the significance of this study. As a suggestion, in regions with high sunflower production, public engagement can be promoted in projects aimed at developing sustainable construction materials. Long-term tests could be conducted to evaluate the material’s performance under various environmental conditions, including humidity, temperature fluctuations, and UV radiation.

Acknowledgment

The authors thank Assoc. Prof. Emre Esener and Assoc. Prof. Oguzhan Demir for their support in the mechanical testing of composite materials.

Conflict of Interest Statement

There is no conflict of interest between the authors.

Statement of Research and Publication Ethics

The study is complied with research and publication ethic.

References

[1] S. Khurana and R. Singh, "Sunflower (Helianthus annuus) seed," in Oilseeds: Health Attributes and Food Applications, Singapore: Springer Singapore, 2020, pp. 123–143.

[2] F. T. Efe, *Ayçiçeği bitkisi (Helianthus annuus L.) saplarının izolasyon levha üretiminde kullanılabilirliğinin araştırılması*, Doktora Tezi, Fen Bilimleri Enstitüsü, 2011.

[3] V. Giannini, C. Maucieri, T. Vamerali, G. Zanin, S. Schiavon, D. M. Pettenella, et al., "Sunflower: From Cortuso's description (1585) to current agronomy, uses and perspectives," *Agriculture*, vol. 12, no. 12, p. 1978, 2022.

[4] M. Stevens, *Formerly USDA, NRCS, National Plant Data Center*, Washington, USA, 2009.

[5] J. Wen, Q. Wang, Q. Jin, and Z. Pan, "Study on the structure, composition and performance of natural polymer," *Functional Materials Letters*, vol. 3, no. 03, pp. 207–212, 2010.

[6] N. Ataman and L. Şık, "Helianthus Annuus L. Comparison of the properties of fibers obtained from the plant by methods of decortication and retting," *Celal Bayar University Journal of Science*, vol. 19, no. 4, pp. 359–366, 2023.

[7] Türkiye İstatistik Kurumu, "Ayçiçeği üretim istatistikleri, 2024." [Online]. Available: https://www.tuik.gov.tr

[8] Bilecik İl Tarım Müdürlüğü, "2023 Yılı İl Brifingi." [Online]. Available: https://bilecik.tarimorman.gov.tr. [Accessed: Nov. 19, 2024].

[9] A. A. Șerbănoiu, C. M. Grădinaru, N. Cimpoeșu, D. Filipeanu, B. V. Șerbănoiu, and N. C. Cherecheș, "Study of an ecological cement-based composite with a sustainable raw material, sunflower stalk ash," *Materials*, vol. 14, no. 23, p. 7177, 2021.

[10] C. Uğur, İ. Bektaş, and A. Tutuş, "Ayçiçeği sapı ile odun karışımından üretilen yongalevhaların bazı fiziksel özelliklerinin belirlenmesi," *Kahramanmaraş Sütçü İmam Üniversitesi Mühendislik Bilimleri Dergisi*, vol. 24, no. 1, pp. 24–33, 2021.

[11] A. N. Sunmaz, U. Doğan, and A. B. İrez, "Ayçiçeği kabuğu takviyeli biyo-epoksi matrisli çevreci ve maliyet etkin kompozitlerin geliştirilmesi ve mekanik karakterizasyonu," *International Journal of Advances in Engineering and Pure Sciences*, vol. 35, no. 4, pp. 494–503, 2023.

[12] H. Temiz, M. M. Maras, and F. Kantarcı, "Polimer katkılı kompozitlerin mekanik ve yalıtım özelliklerinin incelenmesi," *Duzce University Journal of Science and Technology*, vol. 8, no. 2, pp. 1394–1406, 2020.

[13] W. Nimcharoen, C. Sakulkhaemaruethai, and M. Khemkhao, "Bio-based composite from sunflower stalks for building wall panels," *Journal of Renewable Energy and Smart Grid Technology*, vol. 20, no. 1, pp. 45–53, 2025.

[14] S. Zhang, T. Qin, M. Wang, X. Li, S. Liu, T. Li, et al., "Foaming-free sustainable and scalable insulating foams derived from sunflower stalk pith for thermal insulation and sound absorption," *Industrial Crops and Products*, vol. 231, p. 121204, 2025.

[15] P. Bekhta, R. Kozak, V. Gryc, T. Pipíška, J. Sedliačik, R. Reh, et al., "Properties of lightweight particleboard made with sunflower stalk particles in the core layer," *Industrial Crops and Products*, vol. 205, p. 117444, 2023.

[16] İ. Bektas, C. Guler, and H. Kalaycioglu, "Manufacturing of particleboard from sunflower stalks (Helianthus annuus L.) using urea-formaldehyde resin," *Journal of Science and Engineering of KSU, Turkey*, vol. 5, no. 2, pp. 49–56, 2002.

[17] S. Guessasma, K. Abouzaid, S. Belhabib, D. Bassir, and H. Nouri, "Interfacial behaviour in polymer composites processed using droplet-based additive manufacturing," *Polymers*, vol. 14, no. 5, p. 1013, 2022.

[18] F. Şahin and A. Kaymakcı, "Evaluation of the mechanical and physical properties of particleboards manufactured from rice husk," *Artvin Çoruh Üniversitesi Orman Fakültesi Dergisi*, vol. 25, no. 1, pp. 81–85, 2024.

[19] Z. Osman, M. Elamin, E. Ghorbel, and B. Charrier, "Influence of alkaline treatment and fiber morphology on the mechanical, physical, and thermal properties of polypropylene and polylactic acid biocomposites reinforced with kenaf, bagasse, hemp fibers and softwood," *Polymers*, vol. 17, no. 7, p. 844, 2025.

[20] M. D. La Rubia, S. Jurado-Contreras, F. J. Navas-Martos, Á. García-Ruiz, F. Morillas-Gutiérrez, A. J. Moya, et al., "Characterization of cellulosic pulps isolated from two widespread agricultural wastes: cotton and sunflower stalks," *Polymers*, vol. 16, no. 11, p. 1594, 2024.

[21] K. Salasinska, M. Barczewski, R. Górny, and A. Kloziński, "Evaluation of highly filled epoxy composites modified with walnut shell waste filler," *Polymer Bulletin*, vol. 75, no. 6, pp. 2511–2528, 2018.

[22] J. Lu, K. Sheng, J. Chen, X. Ding, Z. Wen, and S. Li, "Influence of particle size and hot-pressing parameters on mechanical properties of bamboo-based composite materials," *Biomimetics*, vol. 10, no. 3, p. 156, 2025.

[23] O. T. Sanya, B. Oji, S. S. Owoeye, and E. J. Egbochie, "Influence of particle size and particle loading on mechanical properties of silicon carbide–reinforced epoxy composites," *The*

International Journal of Advanced Manufacturing Technology, vol. 103, no. 9, pp. 4787–4794, 2019.

[24] H. Ahlatci, E. Candan, and H. Çimenoğlu, "Effect of the particle size on the mechanical properties of 60 vol.% SiCp reinforced Al matrix composites," *International Journal of Materials Research*, vol. 93, no. 4, pp. 330–333, 2022.

[25] F. T. Efe and M. H. Alma, "Investigating some physical properties of composite board, produced from sunflower stalks, designed horizontally," *Ekoloji Dergisi*, vol. 23, no. 90, 2014.

[26] A. K. Chaubey, P. Konda Gokuldoss, Z. Wang, S. Scudino, N. K. Mukhopadhyay, and J. Eckert, "Effect of particle size on microstructure and mechanical properties of Al-based composite reinforced with 10 vol.% mechanically alloyed Mg-7.4% Al particles," *Technologies*, vol. 4, no. 4, p. 37, 2016.

[27] Z. Y. Yang, J. Z. Fan, and Y. Q. Liu, "Effect of the particle size and matrix strength on strengthening and damage process of the particle reinforced metal matrix composites," *Materials*, vol. 14, 2021.

[28] J. Cho, M. S. Joshi, and C. T. Sun, "Effect of inclusion size on mechanical properties of polymeric composites with micro and nano particles," *Composites Science and Technology*, vol. 66, no. 13, pp. 1941–1952, 2006.

[29] J. L. Jordan, J. E. Spowart, M. J. Kendall, B. Woodworth, and C. R. Siviour, "Mechanics of particulate composites with glassy polymer binders in compression," *Philosophical Transactions of the Royal Society A: Mathematical, Physical and Engineering Sciences*, vol. 372, no. 2015, p. 20130215, 2014.

[30] V. Alvarez, A. Vázquez, and C. Bernal, "Fracture behavior of sisal fiber–reinforced starch-based composites," *Polymer Composites*, vol. 26, no. 3, pp. 316–323, 2005.

[31] I. V. Terekhov and E. M. Chistyakov, "Binders used for the manufacturing of composite materials by liquid composite molding," *Polymers*, vol. 14, no. 1, p. 87, 2021.

[32] C. J. Tsenoglou, S. Pavlidou, and C. D. Papaspyrides, "Evaluation of interfacial relaxation due to water absorption in fiber–polymer composites," *Composites Science and Technology*, vol. 66, no. 15, pp. 2855–2864, 2006.

[33] S. Migneault, A. Koubaa, F. Erchiqui, A. Chaala, K. Englund, and M. P. Wolcott, "Effects of processing method and fiber size on the structure and properties of wood–plastic composites," *Composites Part A: Applied Science and Manufacturing*, vol. 40, no. 1, pp. 80–85, 2009.

CHAPTER 3

DEVELOPMENT AND OPTIMIZATION OF A CINNAMON/DOX-LOADED EUDRAGIT S100 POLYMERIC SYSTEM: STATISTICAL DESIGN AND PARTICLE CHARACTERIZATION

Fatma Ceren ÖZBEK[1], Fatma İrem ŞAHİN[2], Nil ACARALI[3]

1 Chemical Engineer, Yildiz Technical University, Department of Chemical Engineering, 34220, Esenler-İstanbul, Türkiye. 0000-0002-3502-143X

2 Chemical Engineer, Yildiz Technical University, Department of Chemical Engineering, 34220, Esenler-İstanbul, Türkiye. 0000-0001-7670-8871

3 Prof.Dr. Yildiz Technical University, Department of Chemical Engineering, 34220, Esenler-İstanbul, Türkiye. 0000-0003-4618-1540 nilbaran@gmail.com

1. INTRODUCTION

Nowadays, breast cancer has been the most often diagnosed cancer in women that is fatal and is the main reason for cancer-related deaths in females. Over the past two decades, research on breast cancer has considerably increased understanding of the disease and has led to the development of more effective therapeutic strategies. Various treatment approaches, including drug therapy, chemotherapy, gene therapy, and theragnostic applications, have been explored for breast cancer management [1–4].

Chemotherapy remains one of the primary treatment modalities; however, conventional anticancer drugs are often associated with significant adverse effects, such as blood abnormalities, alopecia, and neurotoxicity. Compared with single-drug delivery systems, dual-drug delivery systems may enhance therapeutic efficacy by overcoming limitations related to solubility, release behaviour, and systemic toxicity [5–10].

In recent years, various dual drug delivery platforms have been investigated for cancer treatment such as nanoparticles, polymeric micelles, liposomes, dendrimers, Eudragit-based systems, hydrogels, and nanofibers. Among these materials, Eudragit polymers are widely used as pharmaceutical coating agents in oral tablet and capsule formulations due to their pH-responsive properties and ability to provide controlled drug release. In addition to their use as film-coating materials, Eudragit polymers have been increasingly investigated in the development of advanced drug delivery systems [11].

In literature, Eudragit S100-based nanoparticle systems have been developed in which Eudragit S100 serves as the core material, facilitating the self-assembly of micellar structures [12]. In addition, hollow mesoporous silica nanoparticles have been bio conjugated with Epidermal Growth Factor (EGF) to promote efficient and targeted cellular internalization, thereby enhancing the efficiency and specificity of drug delivery [13].

Breast, ovarian, lung, and bladder cancers are among the many cancers that are treated with doxorubicin (DOX), a common anthracycline chemotherapy drug. By intercalating into DNA and blocking topoisomerase II, DOX exhibits anticancer action by stopping the growth of cancer cells. It could be administered intravenously or in liposomal formulations designed to reduce systemic toxicity [14–16].

Cinnamon has also attracted attention due to bioactive and antioxidant properties, and it has been investigated in combination with chemotherapeutic agents to potentially enhance therapeutic performance. Previous studies have demonstrated that formulation optimization using statistical experimental designs, such as the Box–Behnken design, provides an efficient strategy for developing and optimizing nanoparticle-based drug delivery systems [17].

In present study, a cinnamon/DOX-loaded Eudragit S100 polymeric system was developed and optimized using a Box–Behnken experimental design. The effects of doxorubicin, cinnamon, and Eudragit S100 concentrations on the formulation response were statistically evaluated. The optimized formulation was subsequently characterized in terms of particle size distribution and morphological features. The findings provided a statistically supported approach for the development and physicochemical characterization of a dual-loaded polymeric system intended.

2. MATERIALS AND METHODS

2.1 Materials

Cinnamon and doxorubicin (DOX) were used as bioactive components. DOX was obtained from TCI Chemicals. Eudragit S100 was used as the pH-responsive polymeric carrier. A magnetic stirrer (MTOPS MS300HS), an analytical balance (Sartorius CP225D), an optical microscope (SOIF BK5000), and a Zetasizer instrument (Malvern Instruments) were employed for formulation and characterization studies.

2.2. Experimental Method

Prior to experimentation, a Box-Behnken experimental design was formed using Design-Expert software to determine the concentration levels. The experimental setup was carried out according to the coded and actual concentration values provided by the design matrix.

The investigated concentration ranges were as follows: DOX (0.1, 0.2, and 0.3 mg), cinnamon (1, 2, and 3 mg), and Eudragit S100 (10, 20, and 30 mg). For each experimental run, the specified amounts of cinnamon and Eudragit S100 were accurately weighed using an analytical balance and initially mixed.

Under magnetic stirring at 50 °C, the necessary quantity of DOX was dissolved in distilled water. Subsequently, the cinnamon-Eudragit S100 mixture was combined with the DOX aqueous solution under continuous stirring to obtain a homogeneous dispersion.

Following mixing, the resulting suspension was subjected to filtration to separate fractions. The solid fraction retained on the filter paper consisted of polymer-associated components, whereas the filtrate contained the aqueous phase with non-associated materials. The solid portion that remained on the filter paper was dried at room temperature for additional examination. The dried samples were examined to assess their morphological characteristics and particle size distribution (Figure 1).

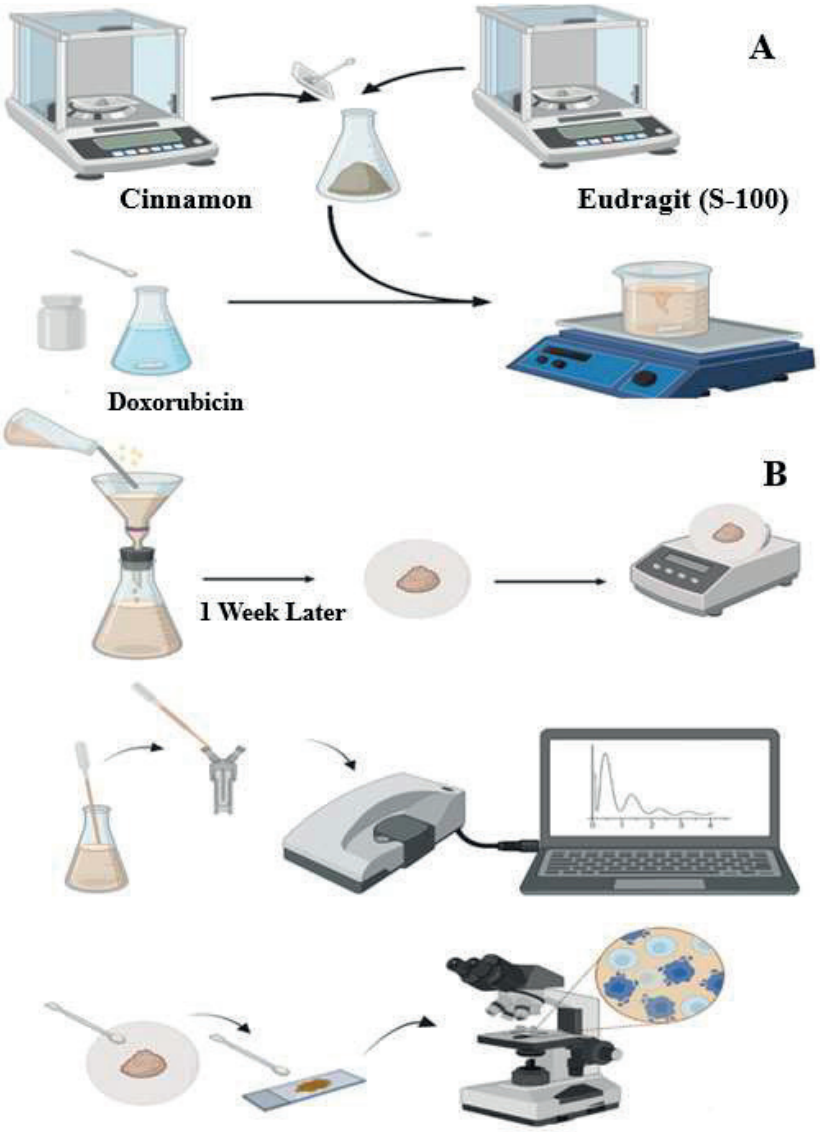

Figure 1. Formulation preparation, filtration, drying, and subsequent particle size and morphological characterization

3. RESULTS AND DISCUSSION

Design-Expert Version 7.0.0 software was used for the form of the experimental design, regression analysis, statistical evaluation, generation of response surface plots, and optimization. A user-defined experimental design generated by Design-Expert was developed and implemented to evaluate the optimization of the drug system and the interactions among the independent variables. In the three-variable design, a total of 17 experimental runs were conducted, including five replications at the center point. Based on preliminary trials, the independent variables and their respective level ranges affecting the drug formulation were

determined as DOX, cinnamon, and Eudragit S100. The amount of doxorubicin remaining on the filter (mg) was defined as the response parameter (R1) (Table 1).

Table 1. Experimental set with Box-Behnken design

NO	DOX	EUDRAGIT (S-100)	CINNAMON	RESPONSE
1	-1	1	0	0.179
2	0	0	0	0.251
3	0	-1	-1	0.122
4	1	0	-1	0.192
5	1	0	1	0.114
6	-1	0	-1	0.128
7	1	1	0	0.217
8	0	0	0	0.246
9	0	0	0	0.239
10	0	-1	1	0.137
11	1	-1	0	0.149
12	0	0	0	0.237
13	0	0	0	0.232
14	0	1	-1	0.188
15	-1	0	1	0.165
16	0	1	1	0.168
17	-1	-1	0	0.132

Based on the optimization results obtained from program, Experiment No. 8 was identified as the optimum formulation. In the developed model, the linear coefficients were designated as A, B, and C, corresponding to doxorubicin, Eudragit-S100, and cinnamon concentrations, respectively. Interaction effects were represented by AB, AC, and BC terms, while the quadratic contributions were expressed as A^2, B^2, and C^2. Model adequacy was supported by a Model F-value of 42.65, demonstrating overall statistical significance. The associated probability indicated that the likelihood of this result arising from random variation was only 0.01%. In the present analysis, A, B, AC, A^2, B^2, and C^2 were identified as significant contributors to the model. Furthermore, the quadratic model's predictive capacity was supported by the Predicted R^2 value (0.8035), which demonstrated acceptable agreement with the Adjusted R^2 value (0.9591) (Table 2).

Table 2. ANOVA Analysis

Source	Sum of Squares	df	Mean Square	F Value	p-value Prob>F	
Model	0.036	9	3.955E-003	42.65	<0.0001	Significant
A-A	5.780E-004	1	5.780E-004	6.23	0.0412	
B-B	5.618E-003	1	5.618E-003	60.59	0.0001	
C-C	2.645E-004	1	2.645E-004	2.85	0.1351	
AB	1.102E-004	1	1.102E-004	1.19	0.3116	
AC	3.306E-003	1	3.306E-003	35.66	0.0006	
BC	3.063E-004	1	3.063E-004	3.3	0.1120	
A^2	6.040E-003	1	6.040E-003	65.15	<0.0001	
B^2	4.832E-003	1	4.832E-003	52.11	0.0002	
C^2	0.012	1	0.012	129.38	<0.0001	
Residual	6.490E-004	7	9.271E-005			
Lack of Fit	4.230E-004	3	1.410E-004	2.5	0.1990	Not significant
Pure Error	2.260E-004	4	5.650E-005			
Cor Total	0.036	16				

The developed model's coefficient of determination (R^2) was 0.9821, meaning that it accounted for 98.21% of the response's overall variation. The expected R^2 value was found to be 0.8035, indicating that the model could estimate about 80.35% of the variability in new data (Table 3).

Table 3. Model Summary

Standard Deviation	9.629E-003	**R^2**	0.9821
Mean	0.18	**Adj R^2**	0.9591
C.V. %	5.29	**Pred R^2**	0.8035
Press	7.121E-003	**Adeq Precision**	16.622

The relatively small difference between R^2 values indicated acceptable consistency and confirmed the satisfactory predictive performance of the model [18-20]. The signal to noise ratio of the model was assessed using the Adequate Precision parameter. In this study, the Adequate Precision value was determined to be 16.622, demonstrating a strong signal and confirming that the model was suitable for predicting responses within the experimental domain (Figure 2).

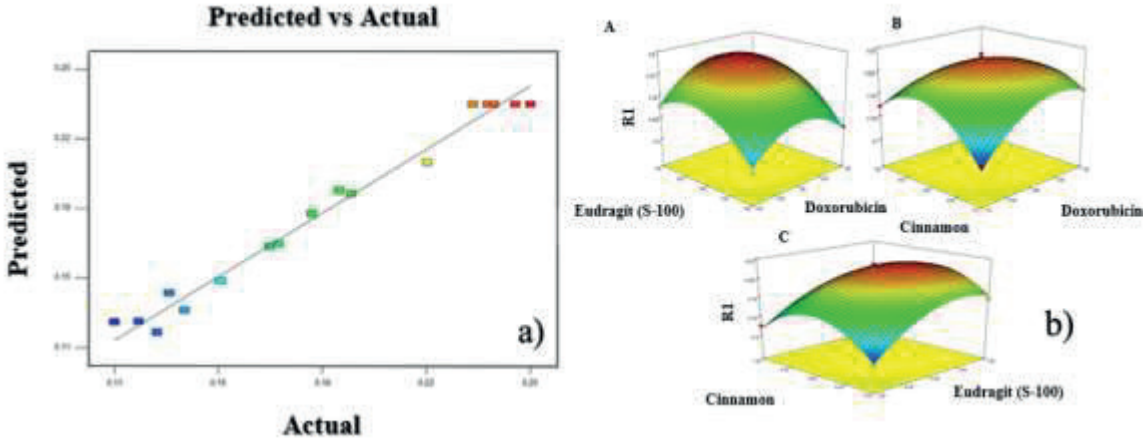

Figure 2. Optimization Results: a) Predicted and Actual R^2 Values**,** b) 3D Response Surface Graphs

The regression model determined for doxorubicin on the filter was as follows Eq. (1):

$$R1=0.24+8.500E\text{-}003\times A+0.027\times B-5.750E\text{-}003\times C+5.250E\text{-}003\times A\times B-0.029\times A\times C-8.750E\text{-}003\times B\times C-0.038\times A^2-0.034\times B^2-0.053\times C^2 \quad (1)$$

Experiment No. 8, identified as the optimum formulation according to the statistical optimization results, was selected for detailed particle size analysis. Particle size analyses of cinnamon, doxorubicin (DOX), Eudragit S100, the solid fraction of Experiment No. 8 retained on the filter paper, and the corresponding liquid fraction were performed using a Malvern Zetasizer based on dynamic light scattering (DLS). In the intensity-based distributions (Figure 3), the solid fraction of Experiment No. 8 (A1) exhibited a relatively narrow and unimodal peak within the submicron range, indicating a uniform particle population after filtration. The liquid fraction (A2) showed a distinct peak in a similar size region, with a slight shift toward smaller diameters compared to the solid fraction, suggesting the presence of more finely dispersed particles in the aqueous phase. The cinnamon sample (A3) displayed a primary dominant peak along with minor secondary peaks, reflecting a limited degree of polydispersity. DOX (A4) demonstrated a sharper and more concentrated distribution profile, consistent with a comparatively uniform particle size. Eudragit S100 (A5) presented a narrow and symmetric distribution, indicating a stable and homogeneous polymer dispersion under the measurement conditions.

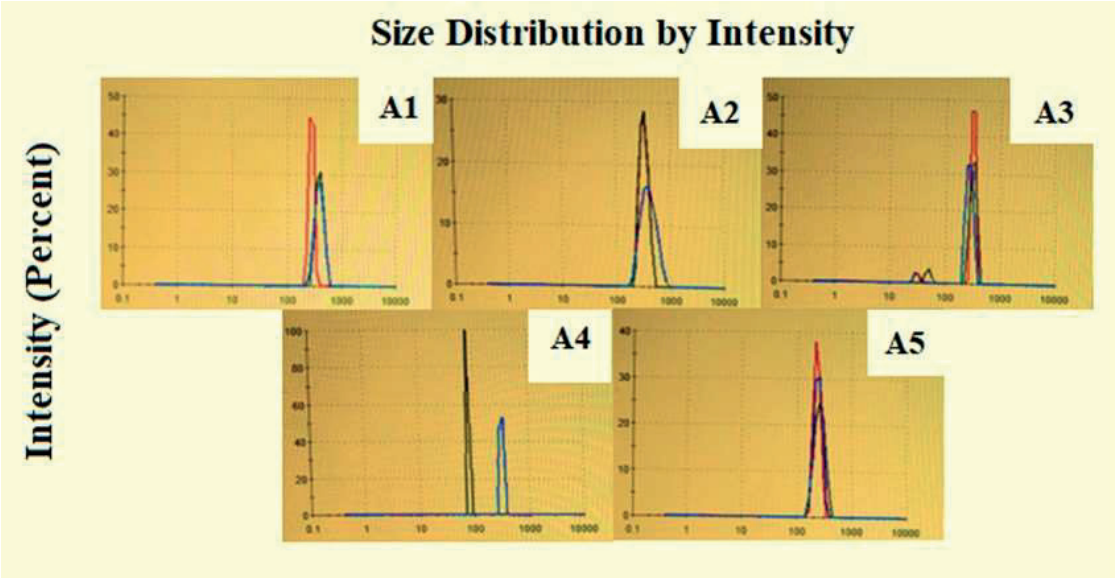

Figure 3. Particle size distribution by intensity obtained using dynamic light scattering A1) solid fraction of optimum retained on the filter paper; A2) liquid fraction of optimum collected in the beaker; A3) cinnamon; A4) doxorubicin (DOX); A5) Eudragit S100

The volume-based size distributions (Figure 4) provided complementary insight into the relative contribution of larger particles within the samples. In these profiles, the solid fraction of the optimized formulation (B1) retained a concentrated and well-defined peak, indicating the dominance of a specific particle size range. The liquid fraction (B2) exhibited a distribution pattern consistent with the intensity-based analysis; however, the contribution of smaller particles was less pronounced due to the volume-weighted calculation method. The cinnamon sample (B3) showed slight peak broadening, suggesting the presence of relatively larger particles contributing more significantly to the overall volume distribution. Doxorubicin (B4) displayed a narrow and distinct peak, supporting the relatively uniform particle size observed in the intensity-based measurements. Eudragit S100 (B5) maintained a compact and symmetric distribution profile, indicative of stable particle dispersion under the measurement conditions. Overall, the agreement between intensity- and volume-based analyses confirmed that the optimized formulation (Experiment No. 8) exhibited a controlled particle size distribution. Clear differences between the solid and liquid fractions following filtration were observed. The consistency between both evaluation approaches supported the reliability of the particle size characterization.

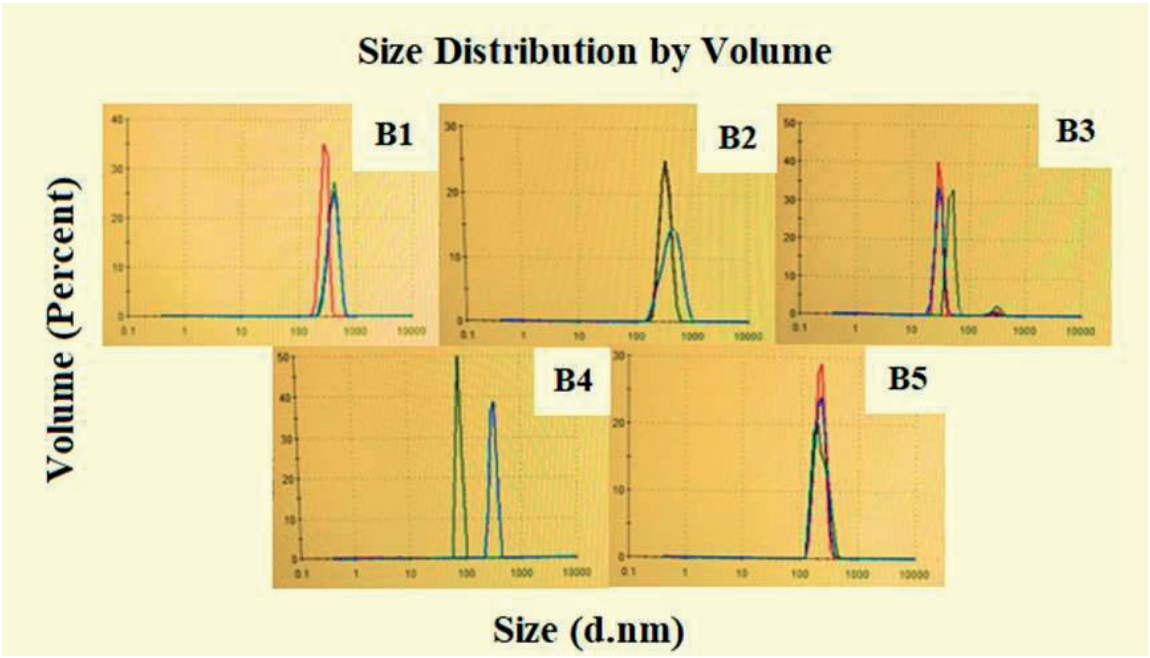

Figure 4. Particle size distribution by volume obtained using dynamic light scattering B1) solid fraction of optimum retained on the filter paper; B2) liquid fraction of optimum collected in the beaker; B3) cinnamon; B4) doxorubicin (DOX); B5) Eudragit S100

The mean particle size of the solid fraction of optimum retained on the filter paper was approximately 250 nm, while the corresponding liquid fraction collected in the beaker exhibited a mean particle size of approximately 300 nm. The cinnamon sample showed a particle size of about 40 nm. Doxorubicin (DOX) exhibited a mean particle size of approximately 170 nm, whereas Eudragit S100 demonstrated a particle size close to 250 nm under the same measurement conditions. Particle size measurements were performed using a Malvern Zetasizer instrument based on dynamic light scattering (DLS), which determines the hydrodynamic diameter of particles by analysing fluctuations in the intensity of scattered light caused by Brownian motion. This technique enabled accurate particle size determination in the nanometer range. Cinnamon, DOX, and Eudragit S100 were analysed individually, and both the solid and liquid fractions of the optimized formulation (Experiment No. 8) were measured separately. The similarity between the particle size of the solid fraction of Experiment No. 8 (≈250 nm) and that of Eudragit S100 suggested the association of DOX within the polymeric matrix [21–24].

Morphological observations were conducted using a SOIF BK5000 optical microscope (Figure 5). Cinnamon, DOX, Eudragit S100, and both the solid and liquid fractions of Experiment No. 8 were examined. The solid fraction of Experiment No. 8 exhibited a distinct morphology

compared to the individual components, appearing larger and darker under microscopic observation. DOX particles appeared comparatively smaller, while Eudragit S100 particles were larger than DOX. Cinnamon showed a tendency toward aggregation. The observed differences in size and morphology supported the formation of a polymer-associated drug system in the optimized formulation. These findings were compatible with previously reported studies [25–28].

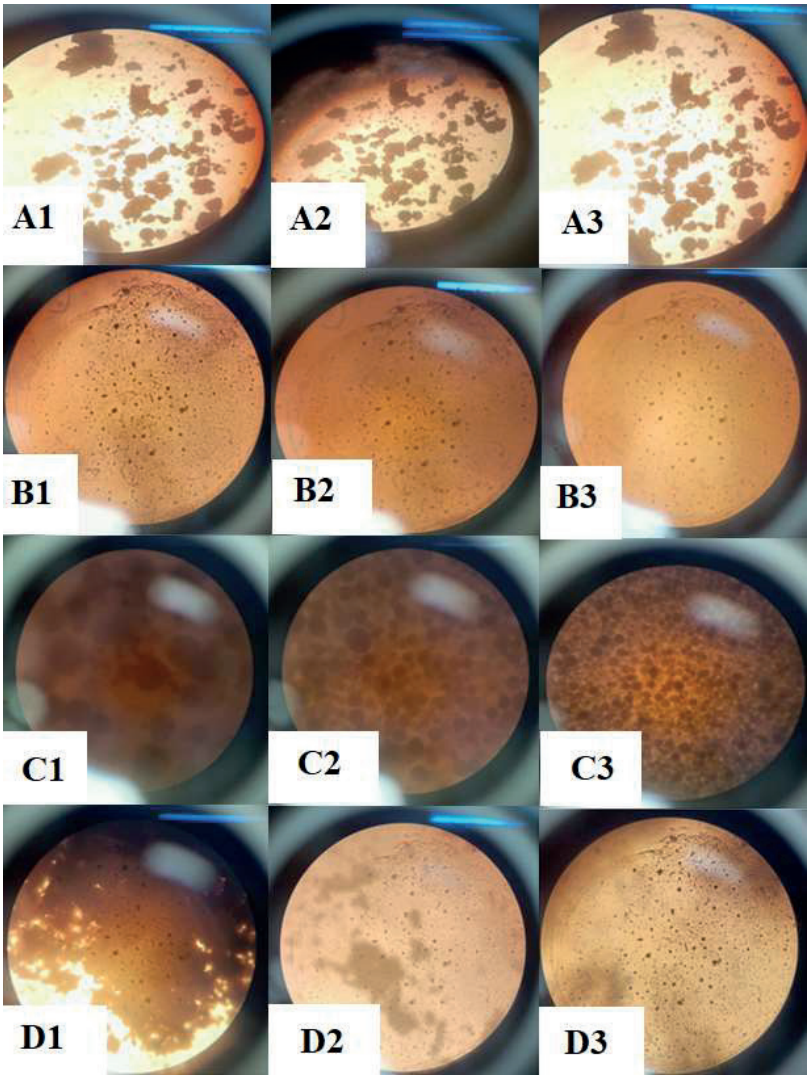

Figure 5. Optical microscopy images of the optimized formulation and individual components at different magnifications. A1–A3: optimum (400×, 200×, and 100×, respectively); B1–B3: doxorubicin (DOX) (400×, 200×, and 100×); C1–C3: Eudragit S100 (400×, 200×, and 100×); D1–D3: cinnamon (400×, 200×, and 100×)

4. CONCLUSION

In this study, a cinnamon/DOX-loaded Eudragit S100 polymeric system was successfully developed and optimized using a Box–Behnken experimental design approach. The effects of doxorubicin, cinnamon, and Eudragit S100 concentrations on the formulation response were systematically evaluated. The high coefficient of determination ($R^2 = 0.9821$) demonstrated strong agreement between the experimental data and the model predictions within the investigated design space. Particle size characterization performed by dynamic light scattering showed that the optimized formulation (Experiment No. 8) exhibited a controlled particle size distribution in the submicron range. Morphological observations further supported the formation of a polymer-associated drug system, with distinguishable differences between the optimized formulation and the individual components. The consistency between statistical modelling and physicochemical characterization confirmed the robustness of the developed system. The application of response surface methodology enabled efficient formulation optimization with a limited number of experimental runs, providing a structured and reproducible strategy for polymeric drug system development. Although biological evaluation was beyond the scope of the present work, the findings offered a statistically supported and characterized platform that could serve as a basis for further pharmaceutical investigations involving dual-loaded polymeric systems.

REFERENCES

[1] Sharma, G., Dave, R., Sanadya, J., Sharma, P., & Sharma, K. (2010). Various types and management of breast cancer: An overview. Journal of Advanced Pharmaceutical Technology Research, 1(2), 109.

[2] Gautam, S., Sharma, K. K., & Amanat, M. (2023). Management of Chemotherapy Induced nausea vomiting (CINV) in breast cancer patients: an imperative factor in patient compliance. Journal of Radiology Nursing, 42(3), 315–320. https://doi.org/10.1016/j.jradnu.2023.04.002

[3] Ofri, A., Elstner, K., Mann, G., Kumar, S., & Warrier, S. (2023). Neoadjuvant chemotherapy in non-metastatic breast cancer: The surgeon's perspective. The Surgeon, *21*(6), 356–360. https://doi.org/10.1016/j.surge.2023.04.001

[4] Tang, H., Wang, R., Liu, W., Xiao, H., Jing, H., Song, F., Guo, S., Li, T., Yi, L., Zhang, Y., Bai, X., & Shang, L. (2023). The influence of nutrition literacy, self-care self-efficacy and social support on the dietary practices of breast cancer patients undergoing chemotherapy: A multicentre study. European Journal of Oncology Nursing, 64, 102344. https://doi.org/10.1016/j.ejon.2023.102344

[5] Liu, P., Xiao, Q., Zhai, S., Qu, H., Guo, F., & Deng, J. (2023). Optimization of drug scheduling for cancer chemotherapy with considering reducing cumulative drug toxicity. Heliyon, 9(6), e17297. https://doi.org/10.1016/j.heliyon.2023.e17297

[6] Al-Shamma, S. A., Zaher, D. M., Hersi, F., Jayab, N. N. A., & Omar, H. A. (2023). Targeting aldehyde dehydrogenase enzymes in combination with chemotherapy and immunotherapy: An approach to tackle resistance in cancer cells. Life Sciences, 320, 121541. https://doi.org/10.1016/j.lfs.2023.121541

[7] Nematullah, M., Hasmatullah, Agnihotri, A., Kumar, S., Husain, A., & Rahman, M. A. (2023). Evaluation of therapeutics' drug monitoring during cancer chemotherapy: A review. Intelligent Pharmacy, 1(3), 157–161. https://doi.org/10.1016/j.ipha.2023.06.005

[8] Yang, Z., Feng, W., Chen, S., Li, X., Yin, B., & Chen, H. (2023). A non-drug chemotherapy-like synergizes with gas-/immunotherapy based on cancer cell membrane camouflage-functionalized nanoplatform. Nano Today, 51, 101912. https://doi.org/10.1016/j.nantod.2023.101912

[9] Farman, M., Batool, M., Nisar, K. S., Ghaffari, A. S., & Ahmad, A. (2023). Controllability and analysis of sustainable approach for cancer treatment with chemotherapy by using

the fractional operator. Results in Physics, 51, 106630. https://doi.org/10.1016/j.rinp.2023.106630

[10] Luiz, M. T., Viegas, J. S. R., Abriata, J. P., Viegas, F., De Carvalho Vicentini, F. T. M., Bentley, M. V. L. B., Chorilli, M., Marchetti, J. M., & Tapia-Blácido, D. R. (2021). Design of experiments (DoE) to develop and to optimize nanoparticles as drug delivery systems. European Journal of Pharmaceutics and Biopharmaceutics, 165, 127–148. https://doi.org/10.1016/j.ejpb.2021.05.011

[11] Rahman, Z., Kohli, K., Khar, R. K., Ali, M., Charoo, N. A., & Shamsher, A. a. A. (2006). Characterization of 5-fluorouracil microspheres for colonic delivery. AAPS PharmSciTech, 7(2), 113-121. https://doi.org/10.1208/pt070247

[12] Patel, N. V., Sheth, N. R., & Mohddesi, B. (2015). Formulation and evaluation of Genistein – a novel isoflavone loaded chitosan and Eudragit® nanoparticles for cancer therapy. Materials Today Proceedings, 2(9), 4477–4482. https://doi.org/10.1016/j.matpr.2015.10.055

[13] She, X., Chen, L., Velleman, L., Li, C., Zhu, H., He, C., Wang, T., Shigdar, S., Duan, W., & Kong, L. (2014). Fabrication of high specificity hollow mesoporous silica nanoparticles assisted by Eudragit for targeted drug delivery. Journal of Colloid and Interface Science, 445, 151–160. https://doi.org/10.1016/j.jcis.2014.12.053

[14] Kurmi, B. D., Paliwal, R., & Paliwal, S. R. (2020). Dual cancer targeting using estrogen functionalized chitosan nanoparticles loaded with doxorubicin-estrone conjugate: A quality by design approach. International Journal of Biological Macromolecules, 164, 2881–2894. https://doi.org/10.1016/j.ijbiomac.2020.08.172

[15] El-Menshawe, S. F., Sayed, O. M., Taleb, H. a. A., Saweris, M. A., Zaher, D. M., & Omar, H. A. (2020). The use of new quinazolinone derivative and doxorubicin loaded solid lipid nanoparticles in reversing drug resistance in experimental cancer cell lines: A systematic study. Journal of Drug Delivery Science and Technology, 56, 101569. https://doi.org/10.1016/j.jddst.2020.101569

[16] Mdlovu, N. B., Lin, K., Weng, M., & Mdlovu, N. V. (2021). Formulation and in-vitro evaluations of doxorubicin loaded polymerized magnetic nanocarriers for liver cancer cells. Journal of the Taiwan Institute of Chemical Engineers, 126, 278–287. https://doi.org/10.1016/j.jtice.2021.06.059

[17] Saraf, A., Dubey, N., Dubey, N., & Sharma, M. (2021). Curcumin loaded Eudragit S100/PLGA nanoparticles in treatment of colon cancer: formulation, optimization, and

in-vitro cytotoxicity study. Indian Journal of Pharmaceutical Education and Research, 55(2s), 428–440. https://doi.org/10.5530/ijper.55.2s.114

[18] Earle, R., & Gadela, V. (2022). Optimization and characterization of self-nanoemulsifying drug delivery system of iloperidone using Box-Behnken design and desirability function. Annales Pharmaceutiques Françaises, 81(1), 40–52. https://doi.org/10.1016/j.pharma.2022.08.008

[19] Kulkarni, P., & Rawtani, D. (2019). Application of Box-Behnken design in the preparation, optimization, and in vitro evaluation of self-assembly–based Tamoxifen- and Doxorubicin-loaded and dual drug–loaded niosomes for combinatorial breast cancer treatment. Journal of Pharmaceutical Sciences, 108(8), 2643–2653. https://doi.org/10.1016/j.xphs.2019.03.020

[20] Shaikh, M. V., Kala, M., & Nivsarkar, M. (2017). Formulation and optimization of doxorubicin loaded polymeric nanoparticles using Box-Behnken design: ex-vivo stability and in-vitro activity. European Journal of Pharmaceutical Sciences, 100, 262–272. https://doi.org/10.1016/j.ejps.2017.01.026

[21] Sonju, J. J., Shrestha, P., Dahal, A., Gu, X., Johnson, W. D., Zhang, D., Muthumula, C. M. R., Meyer, S. A., Mattheolabakis, G., & Jois, S. D. (2023). Lyophilized liposomal formulation of a peptidomimetic-Dox conjugate for HER2 positive breast and lung cancer. International Journal of Pharmaceutics, 639, 122950. https://doi.org/10.1016/j.ijpharm.2023.122950

[22] Ziaei, A. A., Erfan-Niya, H., Fathi, M., & Amiryaghoubi, N. (2023). In situ forming alginate/gelatin hybrid hydrogels containing doxorubicin loaded chitosan/AuNPs nanogels for the local therapy of breast cancer. International Journal of Biological Macromolecules, 246, 125640. https://doi.org/10.1016/j.ijbiomac.2023.125640

[23] Amani, F., Azadi, A., Rezaei, A., Kharazmi, M. S., & Jafari, S. M. (2022). Preparation of soluble complex carriers from Aloe vera mucilage/gelatin for cinnamon essential oil: Characterization and antibacterial activity. Journal of Food Engineering, 334, 111160. https://doi.org/10.1016/j.jfoodeng.2022.111160

[24] Santos, R. B. D., Funguetto-Ribeiro, A. C., Maciel, T. R., Fonseca, D. P., Favarin, F. R., Nogueira-Librelotto, D. R., De Gomes, M. G., Nakamura, T. U., Rolim, C. M. B., & Haas, S. E. (2022). In vivo and in vitro per se effect evaluation of Polycaprolactone and Eudragit® RS100-based nanoparticles. Biomedicine & Pharmacotherapy, 153, 113410. https://doi.org/10.1016/j.biopha.2022.113410

[25] Manhas, P., Sharma, R., Sharma, R., Wangoo, N., Saini, R., Saima, Agrewala, J. N., Sharma, R. K., & Sharma, R. K. (2023). Dox-loaded TPU-PLGA nanoparticles embedded chitosan hydrogel formulation as an effective anti-cancer therapy. Journal of Molecular Liquids, 383, 122170. https://doi.org/10.1016/j.molliq.2023.122170

[26] Deng, T., Luo, D., Zhang, R., Zhao, R., Hu, Y., Zhao, Q., Wang, S., Iqbal, M. Z., & Kong, X. (2022). DOX-loaded hydroxyapatite nanoclusters for colorectal cancer (CRC) chemotherapy: Evaluation based on the cancer cells and organoids. Slas Technology, 28(1), 22–31. https://doi.org/10.1016/j.slast.2022.10.002

[27] Xu, X., Li, Q., Dong, W., Zhao, G., Lu, Y., Huang, X., & Liang, X. (2022). Cinnamon cassia oil chitosan nanoparticles: Physicochemical properties and anti-breast cancer activity. International Journal of Biological Macromolecules, 224, 1065–1078. https://doi.org/10.1016/j.ijbiomac.2022.10.191

[28] Yurtdaş-Kırımlıoğlu, G., Güleç, K., Görgülü, Ş., & Kıyan, H. T. (2021). Oseltamivir phosphate loaded pegylated-Eudragit nanoparticles for lung cancer therapy: Characterization, prolonged release, cytotoxicity profile, apoptosis pathways and in vivo anti-angiogenic effect by using CAM assay. Microvascular Research, 139, 104251. https://doi.org/10.1016/j.mvr.2021.104251